

FAIRNESS FOR THE PEOPLE, BY THE PEOPLE: MINORITY COLLECTIVE ACTION

Anonymous authors

Paper under double-blind review

ABSTRACT

Machine learning models often preserve biases present in training data, leading to unfair treatment of certain minority groups. Despite an array of existing firm-side bias mitigation techniques, they typically incur utility costs and require organizational buy-in. Recognizing that many models rely on user-contributed data, end-users can induce fairness through the framework of Algorithmic Collective Action, where a coordinated minority group strategically relabels its own data to enhance fairness, without altering the firm’s training process. We propose three practical, model-agnostic methods to approximate ideal relabeling and validate them on real-world datasets. Our findings show that a subgroup of the minority can substantially reduce unfairness with a small impact on the overall prediction error.

1 INTRODUCTION

As machine learning (ML) tools become increasingly accessible, more firms deploy them for decision-making. However, ML models often perpetuate societal biases present in their training data, leading to unfair outcomes across demographic groups (Barocas & Selbst, 2016). Moreover, most fairness-preserving learning algorithms incur a non-negligible cost in accuracy or computational resources (Menon & Williamson, 2018; Zhao & Gordon, 2019; Dehdashtian et al., 2024; Sadeghi et al., 2022), which can discourage practical adoption.

Since firms control the ML pipeline, end-users lack access to directly enforce fair treatment. Yet, affected users routinely generate and share data, through clicks, ratings, or other contributions, that is used to train the firm’s models. Such cases, where users collaborate to influence what firms learn, are not uncommon and are well-documented (Sigg et al., 2025). Consequently, if underrepresented minority groups collaboratively alter the data they share, they might be able to steer the learned model towards fairer behavior, even without access to the firm’s training pipeline.

For example, consider a human resources company that makes a profit by filling vacancies and trains ML models on resumes to predict the skills of the candidates. While the majority may have more formal education and college degrees, disadvantaged groups may have informal training or internships. As a result, the ML model does not assign the correct skills to the minority due to their lack of formal education, despite their practical experience. The minority members can react to this injustice by collectively submitting their resumes, but reframing their reported skills, such as sales or management. Appendix A describes other examples where such *collective action* is applicable.

This idea is reminiscent of *pre-processing* fairness techniques (Kamiran & Calders, 2009; Luong et al., 2011; Zemel et al., 2013; Madras et al., 2018), which modify the data before model training. Unlike these prior approaches, which assume centralized control over the data, we consider the setting of *algorithmic collective action* (ACA) (Hardt et al., 2023; Ben-Dov et al., 2024; Baumann & Mender-Dünner, 2024; Sigg et al., 2025; Gauthier et al., 2025), in which a small group of users strategically modifies their own data to influence the correlations learned by the model.

We adapt the *erasure strategy* from Hardt et al. (2023) to reduce predictive correlation between group membership and the target label by relabeling minority samples. The collective is restricted to members of the minority group since minority members are more motivated to join collective action (Saleem et al., 2021; Begeny et al., 2022) and can be efficiently mobilized (McAdam, 1999; Michelson, 2005), while majority-group users may be less inclined to disrupt the status quo. We show that when a classifier is trained on data affected by this form of ACA, standard fairness metrics

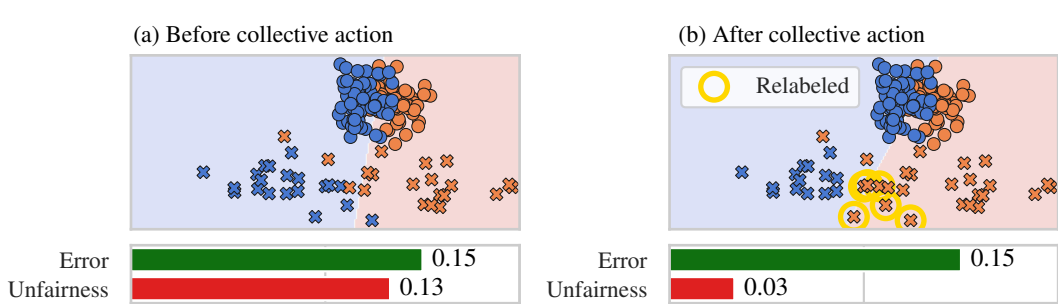


Figure 1: Minority-only collective action can substantially improve fairness. With only 6 label flips, the fairness violation of logistic regression goes down by over 75% with only a negligible increase in prediction error. Circles and crosses represent majority and minority points, respectively.

improve substantially. This improvement is illustrated in Figure 1, where a small minority collective significantly reduces unfairness with minimal impact on prediction error.

The key obstacle in implementing the erasure strategy is that it requires knowledge of each user’s label under a counterfactual group membership. Computing such counterfactual labels exactly would require access to an underlying causal model, which is typically infeasible in practice. To overcome this challenge, we propose three *model-agnostic* methods to estimate the counterfactual labels.

To summarize, our main contributions are: **(1)** We divert from the common firm-side fairness methods and focus on user-side by introducing the setting of **minority-only algorithmic collective action for fairness** in ML (Section 2), and design three algorithms that Pareto-dominate the random-choice baseline. **(2)** Through experiments on benchmark datasets, we demonstrate that these algorithms can **significantly improve fairness metrics** with only a slight accuracy cost and few label flips, and minimal knowledge of majority-group data. **(3)** We investigate **fundamental limitations of minority-only collectives** and provide theoretical results showing that **better representations and better counterfactual approximation methods** can improve these algorithms.

2 COLLECTIVE ACTION FOR FAIRNESS

To establish the connection between fairness and ACA, Section 2.1 first defines the problem setting and how unfairness can be measured. Then, Section 2.2 describes the theoretical framework of ACA and how it can be utilized to mitigate bias. Finally, Section 2.3 formally relates between ACA to group fairness metrics through counterfactual fairness.

2.1 GROUP FAIRNESS FOR CLASSIFICATION

We consider a setting in which a firm uses ML to predict a binary label $y \in \{0, 1\}$. The firm collects data from its users, forming a dataset $\mathcal{D} = \{(x_i, a_i, y_i)\}_{i=1}^n$, where $x_i \in \mathbb{R}^m$ denotes user i ’s feature vector, $a_i \in \{0, 1\}$ is a sensitive attribute indicating binary group membership ($a_i = 0$ for the majority group, $a_i = 1$ for the minority), and $y_i \in \{0, 1\}$ is the true label. We assume the users are drawn independently and identically distributed (i.i.d.) from a distribution \mathbb{P}_0 over $\mathbb{R}^m \times \{0, 1\} \times \{0, 1\}$. The firm trains a classifier $h : \mathbb{R}^m \rightarrow \{0, 1\}$ to minimize the prediction error, defined as

$$\text{Error}(h) = \mathbb{P}[h(x) \neq y]. \quad (1)$$

To do so, the firm minimizes the empirical error on \mathcal{D} via Empirical Risk Minimization (ERM).

In the group-fairness paradigm, the sensitive attribute $a \in \{0, 1\}$ partitions the data into subgroups, and fairness criteria seek to ensure similar outcomes across these groups. Common metrics include statistical parity (SP) (Calders et al., 2009; Dwork et al., 2012) and equalized odds (EqOd) (Hardt et al., 2016). In this work, we focus primarily on violations of EqOd, formally defined as

$$\text{EqOd}(h) = \frac{1}{2} \sum_{z=0,1} |\mathbb{P}[h(x) = 1 | a = 1, y = z] - \mathbb{P}[h(x) = 1 | a = 0, y = z]|, \quad (2)$$

which measures the differences between true positive and false positive rates. Appendix B.1 provides formal definitions and further discussion of these metrics.

ERM-trained models tend to achieve low predictive error, but this often comes at the cost of fairness violations under SP and EqOd (Menon & Williamson, 2018; Zhao & Gordon, 2019; Bardenhagen et al., 2021; Sanyal et al., 2022). Despite significant progress in fairness research, most solutions have traditionally focused on *firm-side* solutions: pre-processing the dataset, in-processing modifications to the training algorithm, or post-processing the classifier’s predictions. These approaches almost always incur errors or additional pipeline complexity, discouraging firms to deploy them in practice.

While most prior work has focused on firm-side solutions, this work shifts the focus to *user-side* methods that do not require the firm’s participation. Since users generate the training data, they can collectively influence the learned model by strategically modifying their own behavior. For instance, consider a digital platform that recommends content to a user based on classifier predicting engagement labels $y_i \in \{\text{will engage, will not engage}\}$. The classifier, trained on historical user interactions, may unintentionally rely on group membership rather than individual preferences when making recommendations for minority members. In response, users can coordinate to alter their interaction patterns, such as clicking on or avoiding certain items. This ACA affects the dataset in a way that steers the learned classifier toward fairer outcomes, and is generally studied under the field of algorithmic collective action (Hardt et al., 2023).

2.2 ALGORITHMIC COLLECTIVE ACTION

In social sciences, *collective action* refers to the coordinated efforts of individuals working together to pursue a shared goal (Olson, 1989; Marwell & Oliver, 1993). Hardt et al. (2023) adapt this notion to ML, proposing that a group of users, termed a collective, can strategically modify their data to align the behavior of a trained classifier h with the collective’s goals. In this formulation, the training distribution is a mixture distribution $\mathcal{D} \sim \mathbb{P}_\alpha = \alpha\mathbb{P}^* + (1 - \alpha)\mathbb{P}_0$, where \mathbb{P}^* and \mathbb{P}_0 are the collective and base distributions, and $\alpha \in [0, 1]$ denotes the proportion of the collective.

Relation to fair representation learning. With user agency over the data, one possible form of ACA for fairness is to modify their features to increase correlation with the label $y = 1$. An analogous firm-side approach is fair representation learning (FRL), which learns a transformation from the input space to a representation space such that ERM leads to a classifier that is both accurate and fair (Zemel et al., 2013; Jovanović et al., 2023). However, a hindrance of FRL in the context of ACA is that the transformation must be applied consistently at inference time, requiring active cooperation from each minority member to transform their features. In contrast, our setting assumes users have control only over the labels and cannot intervene in other parts of the machine learning pipeline.

Erasing a signal. Suppose the collective seeks a classifier that is invariant under a transformation $g : \mathbb{R}^m \rightarrow \mathbb{R}^m$ applied to the features. The success of the collective can be quantified as

$$S(\alpha) = \mathbb{P}_0 [h(g(x)) = h(x)], \quad (3)$$

the probability, under the base distribution, that the classifier’s prediction remains unchanged after applying g to the features. In words, the collective’s goal is to *erase the signal* g : to ensure the classifier behaves identically regardless if the g is applied. Intuitively, if g embeds a feature pattern correlated with group membership (i.e., minority or majority), then achieving invariance under g promotes fairness by reducing the classifier’s dependence on group-identifying information.

To achieve signal erasure, Hardt et al. (2023) propose the collective relabels itself with the most likely label under the transformation g . Formally, the strategy is defined as

$$x, y \rightarrow x, \operatorname{argmax}_{y' \in \{0,1\}} \mathbb{P}_0(y'|g(x)). \quad (4)$$

Since this strategy leaves the features unchanged, it is well-suited for settings where the minority is limited to modify only their labels, such as ours. For ϵ -optimal Bayes classifiers (Definition 2 in Appendix B.2), Hardt et al. (2023) prove the following lower bound for its success

$$S(\alpha) \geq 1 - \frac{2(1 - \alpha)}{\alpha} \cdot \tau - \frac{\epsilon}{(1 - \epsilon)\alpha}, \quad (5)$$

where $\tau = \mathbb{E}_{x \sim \mathbb{P}_0} \left[\max_{y' \in \{0,1\}} |\mathbb{P}_0(y'|x) - \mathbb{P}_0(y'|g(x))| \right]$ captures the sensitivity of y under g .

162
163
164
165
166
167
168
169
170
171
172
173
174
175
176
177
178
179
180
181
182
183
184
185
186
187
188
189
190
191
192
193
194
195
196
197
198
199
200
201
202
203
204
205
206
207
208
209
210
211
212
213
214
215

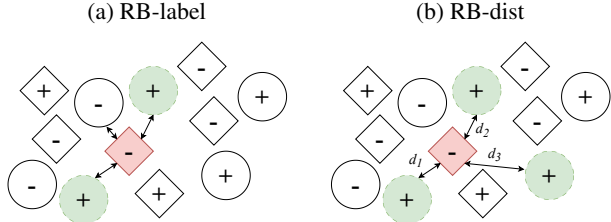


Figure 2: Visualization of KNN scoring methods with $k=3$. The minority is represented by the squares and the majority by circles, marked with a positive “+” or a negative “-” label. **(a) RB-label:** Two of the nearest majority neighbors have a positive label, resulting in the score $s=2$. **(b) RB-dist:** The average distance to the nearest positive majority neighbors results in the score $s=-(d_1+d_2+d_3)/3$.

Note that the strategy in Equation (4) may require some majority members to relabel themselves with the label $y = 0$. Such a change might deter them from participating in the collective action, either because majority members are unwilling to give up their advantage or prefer to maintain the status quo. To avoid this conflict, we restrict the collective to include only minority members. We discuss the implications of this restriction in Section 5.

2.3 COUNTERFACTUAL FAIRNESS

The concept of *counterfactual fairness* (CF) (Kusner et al., 2017; Garg et al., 2019; Wu et al., 2019) bridges between signal erasure success to group fairness. To introduce this idea, assume that a sample x is generated by a causal model, in which the group membership A is a causal parent. Then a classifier h is counterfactually fair if its predictions are invariant to interventions on the group membership, i.e., $h(x) = h(x_{A \leftarrow a'})$ for any a' , where $x_{U \leftarrow u}$ denotes an intervention on a causal parent U of a sample x . In certain causal contexts, CF implies or aligns with group fairness criteria such as SP or EqOd (Anthis & Veitch, 2023). Therefore, if ACA induces a counterfactually fair classifier, it may also induce a fair classifier under SP or EqOd.

As focus is on fairness for the minority, we relax the original definition of CF (Kusner et al., 2017). **Definition 1.** A classifier h is *minority-focused counterfactually fair* if under any context $X = x$,
$$\mathbb{P}_0(h(x_{A \leftarrow a}) = y | X = x, A = 1) = \mathbb{P}_0(h(x_{A \leftarrow a'}) = y | X = x, A = 1), \tag{6}$$
 for any value a' attainable by A .

By this definitions, changing the group membership of a minority individual, in a counterfactual sense, has no effect on the classifier’s prediction. ACA can theoretically enforce such fairness by applying the erasure strategy from Equation (4) with the counterfactual signal $g(x) = x_{A \leftarrow 0}$, which replaces a minority individual with its majority-group counterfactual. This ACA aligns the signal erasure success from Equation (3) with minority-focused counterfactual fairness from Definition 1. The following proposition, proved in Appendix C.1, formalizes this alignment.

Proposition 1. A Bayes classifier trained on \mathbb{P}_α is minority-focused counterfactually fair if and only if the success of a minority collective is $S = 1$.

This result directly connects between ACA theory to fairness. Thus, perfect success of the collective is equivalent to achieving minority-focused counterfactual fairness.

3 APPROXIMATING THE COUNTERFACTUAL LABEL

This section describes how a minority collective can approximate a signal-erasure strategy to promote fairness in practice. While the theory of signal erasure has been studied before (Hardt et al., 2023; Gauthier et al., 2025), prior work lacks empirical evaluation. In this paper, we present the first practical algorithm for signal erasure and provide experimental results in Section 4. As discussed in Section 2.3, a suitable signal to erase is $g(x) = x_{A \leftarrow 0}$, where each collective member relabels themselves according to Equation (4).

However, end-users lack access to the true causal model and cannot compute the counterfactual labels directly. To address this limitation, we propose to assign each collective member i a score s_i ,

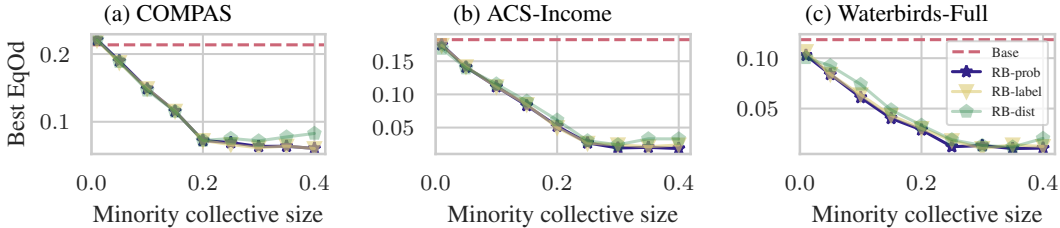


Figure 3: The lowest EqOd violation a collective can achieve greatly improves as the collective size increases, up to a certain point. Each point is a mean of 10 runs, with the standard deviation being smaller than the markers. In all the datasets we experimented on, the lowest EqOd violation converges around $\alpha = 0.3$. Additional results are presented in Figure 11 in the appendix.

which serves as a proxy for the likelihood that they would receive the label $y = 1$ if they belonged to the majority. Given a budget of M label flips, the collective selects the M members with the highest scores; these individuals flip their labels from $y = 0$ to $y = 1$. The budget M controls the accuracy–fairness tradeoff, where a higher budget typically leads to better fairness, but higher error.

We introduce three scoring functions, each capturing a different notion of similarity to majority users:

1. **Rank by probability (RB-prob):** Train a regressor $f : \mathbb{R}^m \rightarrow \mathbb{R}$ on exclusively majority data ($a = 0$) to estimate the probability $\mathbb{P}(Y = 1|X = x)$ of having the label $y = 1$. Each collective member i receives a score based on the model’s prediction:

$$s_i = f(x_i). \quad (7)$$

2. **Rank by label (RB-label):** For each collective member i , identify the set K_i of their k nearest majority neighbors using Euclidean distance. The score is the number of neighbors with the label $y = 1$:

$$s_i = \sum_{j \in K_i} \mathbf{1}\{y_j = 1\}. \quad (8)$$

3. **Rank by distance (RB-dist):** Restrict the neighbors set K_i to only majority users with the label $Y = 1$. The score is the negative mean Euclidean distance to these neighbors:

$$s_i = -\frac{1}{k} \sum_{j \in K_i} \|x_i - x_j\|_2. \quad (9)$$

Intuitively, RB-prob assigns a higher score where a classifier trained solely on majority data predicts a higher likelihood of the label $y = 1$. RB-label scores collective members according to the frequency of $y = 1$ among their majority neighbors, while RB-dist prioritizes those who are closer majority users with $y = 1$. Figure 2 provides visualizations for RB-label and RB-dist.

4 EXPERIMENTAL RESULTS

This section evaluates the performance of our methods. We compare the three methods, RB-label, RB-dist, RB-prob, against a random baseline that flips $y = 0$ labels to $y = 1$ for M randomly selected collective members. We conducted experiments on the tabular datasets COMPAS (Mattu et al., 2016), Adult (Becker & Kohavi, 1996), HSLs (Jeong et al., 2022), ACS-Income (Ding et al., 2021), the image dataset Waterbirds (Sagawa et al., 2020) and the text dataset CivilComments (Borkan et al., 2019). For Waterbirds, we use features extracted from a pre-trained *ResNet-18* (denoted Waterbirds-Full) and for CivilComments, we used the extracted features from Hugging Face’s pre-trained *bert-base-uncased* model (denoted CivilComments-Full). In addition to the complete features of Waterbirds and CivilComments, we also include experiments on the PCA features, with 85 components for Waterbirds (denoted Waterbirds-PCA) and 100 components for CivilComments (denoted CivilComments-PCA). Details on the datasets and the pre-processing are provided in Appendix D.1.

All reported metrics are computed on a fixed test set, without any ACA, and averaged over 10 independent runs for each method described in Section 3. In each run, we randomly selected a minority collective to apply the method. For the KNN-based methods, we tuned the neighborhood

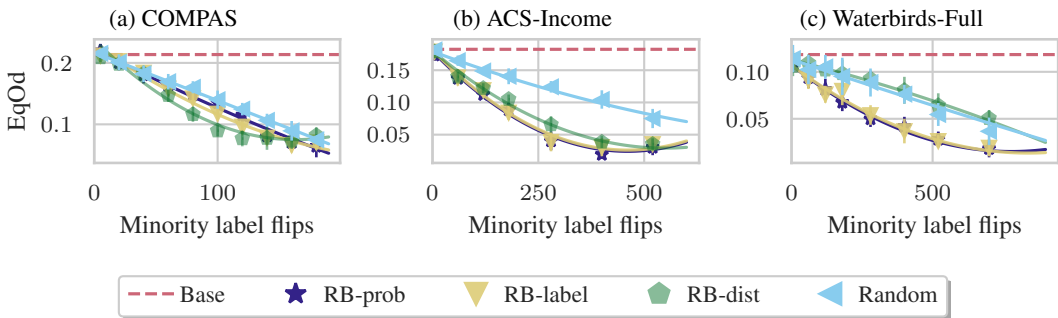


Figure 4: Our proposed methods are consistently more efficient than randomly flipping labels, requiring less label flips to attain the same level of EqOd. Each marker is the mean of 10 random runs with a specific number of label flips. The standard deviation is presented by the error bars. The dashed line shows the mean EqOd for a classifier trained on the dataset without collective action.

size k using a 15% validation split from the train set, optimizing for EqOd and SP. Finally, we trained a gradient-boosted decision tree on each modified train set. More technical details are given at Appendix D.2 and the complete set of results can be found in Appendix E.2.

Importance of collective size While the number of label flips M is the primary factor for balancing between accuracy and fairness, the size of the collective, α , also plays a role. In addition to bounding the possible number of flips, increasing α also expands the candidate pool from which the most effective labels to flip can be selected. To measure this effect, the experiments included a range of α values, each tested with multiple values of M . For each α , we define the best achievable EqOd as the minimum EqOd across all tested values of M . As shown in Figure 3, increasing α improves the best achievable EqOd until saturating around $\alpha = 0.3$. We fix this value for all remaining experiments.

Flipping cost Since each method scores candidates differently, they may also vary in efficiency, that is, the number of label flips required to achieve a given level of fairness. To evaluate efficiency, Figure 4 plots EqOd as a function of number of label flips M , where lower curves indicate more efficient methods. The random baseline consistently yields the worst EqOd across all values of M , highlighting the value of informed relabeling algorithms. However, no single method dominates the others in all settings: While RB-prob and RB-label often outperform the other methods, RB-dist can surpass them in specific cases (e.g., Figure 4a), or perform comparably to the random baseline in others (Figure 4c). These results suggest that a well-chosen scoring function enables the collective to achieve a desired level of fairness with fewer label flips, reducing the “cost” of ACA and mitigating the accuracy loss from excessive relabeling.

Interestingly, beyond a certain number of flips, EqOd begins to increase, indicating that excessive flipping can shift unfairness from the minority to the majority. This upturn reflects the fundamental limits of minority ACA for fairness, a point we elaborate on in Section 5.

Partial knowledge of the majority In all previous experiments, we assumed that the collective has full access to the majority data to estimate the counterfactual labels. Here we investigate the performance of our methods when limiting this knowledge. To visualize the fairness-error tradeoff, we measure the error and EqOd for a range of label flips, yielding a set of pairs (Error, EqOd). This set forms a Pareto front, representing the tradeoff. A Pareto front is said to *dominate* another if it lies entirely to the left (lower error) and below (lower unfairness) of the other. The Pareto fronts in Figure 5 exhibit that a collective employing RB-prob, when restricted to only 10 majority members, performs similarly as a collective with full knowledge. While the Pareto fronts remain similar, limited majority knowledge can increase the number of required flips. This is evident when comparing to the zero-knowledge scenario, designated as random in Figure 4. This finding implies that the fewer flips the collective is allowed, the more important it is to have access to the majority data.

5 LIMITATIONS OF MINORITY COLLECTIVE ACTION

Previous work on ACA assumes that the collective is uniformly sampled from the distribution \mathbb{P}_0 and that the collective has a perfect oracle for the conditional distribution $\mathbb{P}_0(Y|X)$. Yet, our method

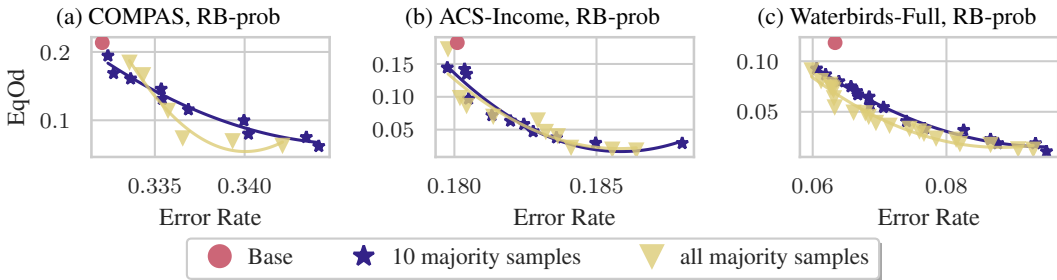


Figure 5: Limiting the knowledge of the collective about the majority does not significantly harm the Pareto front. Each point is the mean of 10 runs and the curves are fitted to guide the eye.

restricts collective participation to minority members and approximates this conditional distribution. Those differences introduce limitations to the existing theory, which we analyze in this section.

Collective restricted to the minority. As mentioned above, we focus on collectives composed solely of minority members, unlike prior work. This restriction expresses scenarios in which majority members lack incentives to support changes that would benefit the minority, and instead prefer to preserve the status quo. Naturally, this limitation reduces the collective’s impact. Consider a binary classification task on the two-dimensional 4-Gaussian mixture model \mathbb{P}_{4GMM} where each Gaussian belongs to a distinct combination of label and group membership, as illustrated in Figure 6. Each label consists of a large majority subgroup and a significantly smaller minority subgroup. We can then state the following informal result about the EqOd fairness violation of ERM.

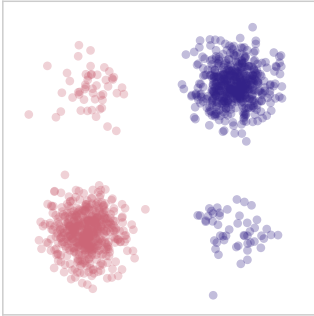


Figure 6: The distribution \mathbb{P}_{4GMM} used in Proposition 2. The color signifies the label, and the density shows the group membership.

Proposition 2 (Informal). Consider the dataset \mathbb{P}_{4GMM} , where every minority point participates in the ACA by flipping all $y = 0$ labels to $y = 1$. Then, under sufficiently separable clusters, with high probability, the EqOd of the ERM classifier minimizing the logistic loss will asymptotically approach 0.5.

The formal Proposition 5 is provided in Appendix C.2 along with all necessary assumptions, which holds for a broader family of distributions and can be extended to any dimensionality \mathbb{R}^d using techniques similar to those in Chaudhuri et al. (2023). Although Proposition 2 is not a formal lower bound, it emphasizes an important limitation: ACA restricted to the minority cannot generally achieve perfect fairness, even under very advantageous conditions involving a maximum-sized collective, a strong strategy, and a disregard for accuracy. This limitation stands in contrast to standard firm-side bias mitigation methods, which in principle, achieve perfect fairness. There are several reasons why relabeling alone may not be enough to get perfect fairness. For one, relabeling according to the counterfactual implicitly assumes that the label is determined by the same features across the majority and minority, but this assumption is not valid under certain distribution shift between the groups. To illustrate, consider a firm training a classifier to screen candidates for a managerial position. Majority members may be more educated, while minority members may have more hands-on experience rather than formal education. In this case, a counterfactual label associated with the majority is disjointed from the features associated with the features, rendering the signal erasure strategy irrelevant. Future work could study this problem and determine when it is beneficial to change the features as well.

We empirically corroborate the findings of Proposition 2 on real world datasets by examining the fairness–accuracy tradeoff of several fair learning methods. Figure 7 compares the Pareto fronts of RB-prob, one of our minority ACA methods, with established firm-side methods. We observe that the lowest fairness violation achievable by RB-prob is greater than that of the firm-side approaches. However, the firm-side methods are able to arrive at perfect fairness only at a cost of prohibitively high prediction error. But, inspecting the region where the error is small compared to the base classifier, the fairness of RB-prob is comparable to that of the firm-side methods.

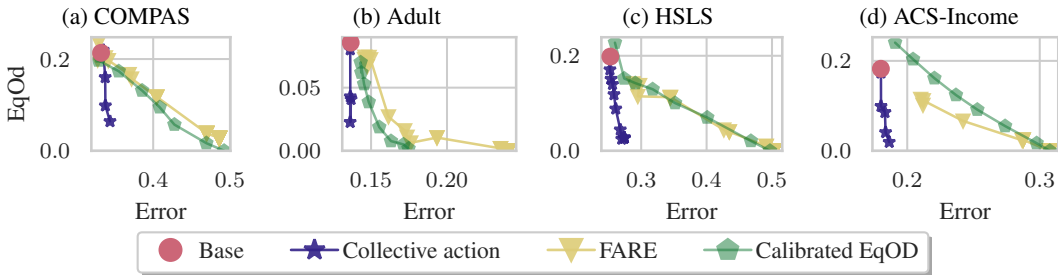


Figure 7: User-side method cannot achieve perfect fairness, while the firm-side pre-processing method FARE Jovanović et al. (2023) and the post-processing method calibrated equalized odds Pleiss et al. (2017) attain 0 EqOd with large error. However, RB-prob’s fairness is better than the base classifier, with a smaller error than the firm-side methods.

Estimating counterfactuals. In Section 3 we proposed methods to estimate which individuals would receive a counterfactual label that is different than their original label. However, the success lower bound in Equation (5) assumes perfect knowledge of \mathbb{P}_0 and of the underlying causal model. To account for the estimation error, we model the collective’s prediction as the output of an algorithm $\mathcal{A}(x) \approx \mathbb{P}_0 \max_y (y|x_{A \leftarrow 0})$ that has an error rate ρ , defined as

$$\rho := \mathbb{P}_0(\mathcal{A}(x) \neq \arg \max_y \mathbb{P}_0 [y'|g(x)]). \quad (10)$$

Given this definition, we derive the following lower bound on success, proved in Appendix C.3.

Proposition 3. *With algorithm $\mathcal{A}(x)$ with label error ρ , the success of the collective is bounded by*

$$S(\alpha) \geq 1 - \frac{2(1-\alpha)}{(1-2\rho)\alpha} \tau - \frac{\epsilon}{(1-\epsilon)(1-2\rho)\alpha}. \quad (11)$$

This bound recovers Equation (5) when $\rho = 0$, but higher values of the error ρ worsen the bound. Next, we show how to use FRL to reduce the error ρ , thereby improving the lower bound.

Impact of feature representations Since the methods RB-label and RB-dist rely on KNN, their performance is sensitive to the choice of distance metric and feature representation. In our main experiments, we used Euclidean distance in the original feature space, which is convenient but could be suboptimal. Here, we explore whether FRL can learn a more suitable representation space for KNN. A *fair representation* maps the data into a space where the group-based bias is removed while preserving informative features. Intuitively, such representations may help RB-label and RB-dist to better estimate the counterfactual labels. To formalize this intuition, we consider predicting the counterfactual label of minority points using a 1-NN classifier on majority data, i.e., assigning each minority point the label of its nearest neighbor in the majority. In settings where the minority is distributed differently than the majority (e.g., \mathbb{P}_{4GMM}), this task can be challenging. The following informal result compares the error of 1-NN in the original features space to its error in FRL.

Proposition 4 (Informal). *Let data be drawn from \mathbb{P}_{4GMM} , and ρ_{plain} denote the error of a 1-NN classifier that assigns the label of the nearest majority neighbor in the original feature space. Then there exists a fair representation in which a 1-NN classifier achieves error ρ_{FRL} such that, asymptotically with respect to the dataset size, $\rho_{FRL} \leq \rho_{plain}$.*

The formal statement, Theorem 1 can be found in Appendix C.4. The result suggests that FRL can reduce the counterfactual label error ρ of RB-label and RB-dist, consequently improving the lower bound of the collective’s success according to Proposition 3. Empirically, Figure 8 indicates that applying FARE (Jovanović et al., 2023) before the KNN step improves the Pareto front for RB-dist. On the other hand, methods that rely purely on predictive information, such as RB-prob, can perform worse, due to FRL inadvertently removing features predictive of the class label.

6 RELATED WORK

Optimizing for fairness often comes at the cost of reduced classification accuracy, leading to the well-documented accuracy–fairness tradeoff (Menon & Williamson, 2018; Zhao & Gordon, 2019;

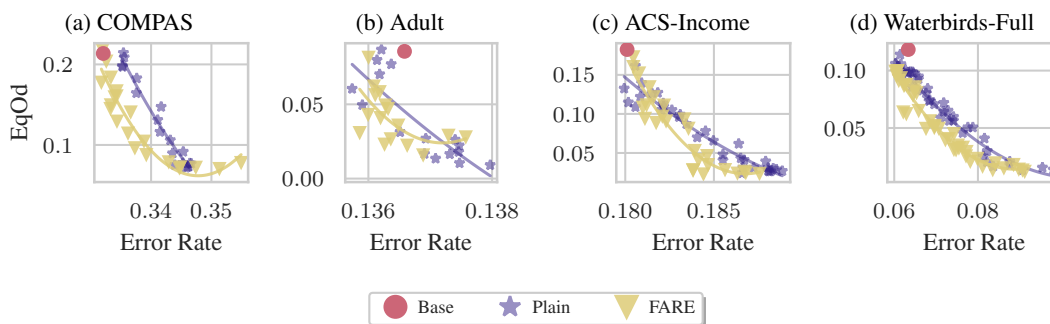


Figure 8: The Pareto fronts for using a fair representation when computing the KNN for RB-dist dominate the Pareto fronts for KNN computed on untransformed features. The blue stars represent the KNN without transforming the data, and the yellow triangles represent the KNN when the data is transformed using FARE Jovanović et al. (2023). The lines are fitted to guide the eye.

Dehdashtian et al., 2024; Sadeghi et al., 2022). In response, previous work has proposed fairness interventions at different stages of the ML pipeline: pre-processing methods modify the training data before learning (Kamiran & Calders, 2009; Luong et al., 2011; Zemel et al., 2013; Jovanović et al., 2023), in-processing methods adjust the learning algorithm itself (Agarwal et al., 2018; Nam et al., 2020; Sagawa et al., 2020; Liu et al., 2021), and post-processing methods correct the predictions of a trained (unfair) classifier (Hardt et al., 2016; Alghamdi et al., 2022; Tifrea et al., 2024; Cruz & Hardt, 2024). A firm can introduce any of these categories into its pipeline, while users, who control only their data can only partially implement pre-processing methods. However, as mentioned in Section 2.2, using feature-changing pre-processing methods such as fair representation learning (Zemel et al., 2013; Jovanović et al., 2023) demand changing those features during inference time as well.

Still, some pre-processing methods change only the labels, similarly to our proposed collective action. The method by Luong et al. (2011) compares between the minority KNN and majority KNN and flip the labels according to the difference of positive labels between the two groups of neighbors. This method resembles RB-label, with the difference that RB-label examines only the majority KNN in order to approximate the counterfactual. The approach of Kamiran & Calders (2009) trains a regressor to predict $y = 1$ outcome probabilities, and flip the label of minority members with $y = 0$ labels and high probability according to the regressor to have $y = 1$, and similarly flip majority $y = 1$ labels to $y = 0$. Flipping from both groups supposedly preserves the error of the classifier. Our method RB-prob differs by training the regressor only on the majority to better approximate the counterfactuals. Since this approach requires flipping the labels of majority members as well, it cannot be completely adopted by the collective. In Appendix E.1 we compare the between RB-prob to CND and KDP, and find that our method is more efficient in terms of number of label flips.

7 CONCLUSION

This work demonstrates that user-side methods can effectively reduce unfairness in machine learning. While much of the existing fairness research focused on firm-side methods, these often come at a cost that may not be worth to the firm. This catch emphasizes the importance of studying user-side approaches for bias mitigation. We show empirically that ACA can considerably reduce unfairness in a variety of datasets, though not completely. Importantly, we also examine the limitations of a minority being composed of only minority members, and how the success is affected by approximating the counterfactual labels. Our proposed methods require the collective to relabel themselves, which often comes with a price, as the users have to go against their true nature. However, as has been studied on real world cases, minority members willingly participate in collective action to benefit their demographic, after being encouraged by their community (Begeny et al., 2022) or by the media (Saleem et al., 2021) and efficiently mobilized in large-enough scales (McAdam, 1999; Michelson, 2005).

We also note that in general, ACA methods can be exploited by malicious parties seeking self-gain or harming other communities, and it is important to discuss these limitations and possibly regulate them. Overall, this paper shows a practical use case of collective action in the hopes of sparking further research into applications of ACA and user-side methods for social good.

486 REPRODUCIBILITY STATEMENT
487

488 We publish all code necessary to reproduce the experiments in the paper. The details of how we
489 pre-process the datasets are described in Appendix D.1 and also contained in our codebase. Finally,
490 we provide the training details in Appendix D.2.
491

492 LLM USAGE STATEMENT
493

494 We used ChatGPT to rephrase some sentences and find better words to improve the reading flow of
495 the paper.
496

497 REFERENCES
498

- 499 Alekh Agarwal, Alina Beygelzimer, Miroslav Dudik, John Langford, and Hanna Wallach. A
500 reductions approach to fair classification. In *Proceedings of the 35th International Conference on*
501 *Machine Learning*, volume 80, pp. 60–69. PMLR, 2018.
502
- 503 Wael Alghamdi, Hsiang Hsu, Haewon Jeong, Hao Wang, Peter Michalak, Shahab Asoodeh, and
504 Flavio Calmon. Beyond adult and COMPAS: Fair multi-class prediction via information projection.
505 In *Advances in Neural Information Processing Systems*, volume 35, pp. 38747–38760. Curran
506 Associates, Inc., 2022.
- 507 Jacy Anthis and Victor Veitch. Causal context connects counterfactual fairness to robust prediction
508 and group fairness. In *Advances in Neural Information Processing Systems*, volume 36, pp.
509 34122–34138. Curran Associates, Inc., 2023.
- 510 Vincent Bardenhagen, Alexandru Tifrea, and Fan Yang. Boosting worst-group accuracy without
511 group annotations. In *NeurIPS 2021 Workshop on Distribution Shifts: Connecting Methods and*
512 *Applications*. OpenReview, 2021.
513
- 514 Solon Barocas and Andrew D. Selbst. Big data’s disparate impact. *California Law Review*, 104(3):
515 671–732, 2016.
- 516 Joachim Baumann and Celestine Mendler-Düner. Algorithmic Collective Action in Recommender
517 Systems: Promoting Songs by Reordering Playlists. In *Advances in Neural Information Processing*
518 *Systems*, volume 37, pp. 119123–119149. Curran Associates, Inc., 2024.
- 519 Barry Becker and Ronny Kohavi. Adult. UCI Machine Learning Repository, 1996.
520
- 521 Christopher T. Begeny, Jolien van Breen, Colin Wayne Leach, Martijn van Zomeren, and Aarti Iyer.
522 The power of the Ingroup for promoting collective action: How distinctive treatment from fellow
523 minority members motivates collective action. *Journal of Experimental Social Psychology*, 101:
524 104346, 2022.
- 525 Omri Ben-Dov, Jake Fawkes, Samira Samadi, and Amartya Sanyal. The Role of Learning Algorithms
526 in Collective Action. In *Proceedings of the 41st International Conference on Machine Learning*,
527 volume 235, pp. 3443–3461. PMLR, 2024.
528
- 529 Daniel Borkan, Lucas Dixon, Jeffrey Sorensen, Nithum Thain, and Lucy Vasserman. Nuanced
530 Metrics for Measuring Unintended Bias with Real Data for Text Classification. In *Companion*
531 *Proceedings of The 2019 World Wide Web Conference*, pp. 491–500. Association for Computing
532 Machinery, 2019. ISBN 978-1-4503-6675-5.
- 533 Toon Calders, Faisal Kamiran, and Mykola Pechenizkiy. Building Classifiers with Independency
534 Constraints. In *2009 IEEE International Conference on Data Mining Workshops*, pp. 13–18, 2009.
535
- 536 Kamalika Chaudhuri, Kartik Ahuja, Martin Arjovsky, and David Lopez-Paz. Why does throwing
537 away data improve worst-group error? In *Proceedings of the 40th International Conference on*
538 *Machine Learning*, volume 202, pp. 4144–4188. PMLR, 2023.
- 539 André Cruz and Moritz Hardt. Unprocessing seven years of algorithmic fairness. In *The Twelfth*
International Conference on Learning Representations, 2024.

- 540 Sepehr Dehdashtian, Bashir Sadeghi, and Vishnu Naresh Boddeti. Utility-fairness trade-offs and
541 how to find them. In *Proceedings of the IEEE/CVF Conference on Computer Vision and Pattern
542 Recognition (CVPR)*, pp. 12037–12046, 2024.
- 543
- 544 Frances Ding, Moritz Hardt, John Miller, and Ludwig Schmidt. Retiring Adult: New Datasets for
545 Fair Machine Learning. In *Advances in Neural Information Processing Systems*, volume 34, pp.
546 6478–6490. Curran Associates, Inc., 2021.
- 547 Cynthia Dwork, Moritz Hardt, Toniann Pitassi, Omer Reingold, and Richard Zemel. Fairness through
548 awareness. In *Proceedings of the 3rd Innovations in Theoretical Computer Science Conference*, pp.
549 214–226. Association for Computing Machinery, 2012. ISBN 978-1-4503-1115-1.
- 550
- 551 Sahaj Garg, Vincent Perot, Nicole Limtiaco, Ankur Taly, Ed H. Chi, and Alex Beutel. Counterfactual
552 fairness in text classification through robustness. In *Proceedings of the 2019 AAAI/ACM Conference
553 on AI, Ethics, and Society*, pp. 219–226. Association for Computing Machinery, 2019. ISBN
554 978-1-4503-6324-2.
- 555 Etienne Gauthier, Francis Bach, and Michael I. Jordan. Statistical collusion by collectives on learning
556 platforms. In *Forty-Second International Conference on Machine Learning*, 2025.
- 557
- 558 Moritz Hardt, Eric Price, and Nathan Srebro. Equality of Opportunity in Supervised Learning. In
559 *Proceedings of the 30th International Conference on Neural Information Processing Systems*, pp.
560 3323–3331, 2016.
- 561
- 562 Moritz Hardt, Eric Mazumdar, Celestine Mendler-Dünner, and Tijana Zrnic. Algorithmic Collective
563 Action in Machine Learning. In *Proceedings of the 40th International Conference on Machine
564 Learning*, volume 202, pp. 12570–12586, 2023.
- 565
- 566 Haewon Jeong, Hao Wang, and Flavio P. Calmon. Fairness without Imputation: A Decision Tree
567 Approach for Fair Prediction with Missing Values. *Proceedings of the AAAI Conference on
Artificial Intelligence*, 36(9):9558–9566, 2022.
- 568
- 569 Nikola Jovanović, Mislav Balunovic, Dimitar Iliev Dimitrov, and Martin Vechev. FARE: Provably
570 Fair Representation Learning with Practical Certificates. In *Proceedings of the 40th International
571 Conference on Machine Learning*, pp. 15401–15420. PMLR, 2023.
- 572
- 573 Faisal Kamiran and Toon Calders. Classifying without discriminating. In *Control and Communication
2009 2nd International Conference on Computer*, pp. 1–6, 2009.
- 574
- 575 Matt J Kusner, Joshua Loftus, Chris Russell, and Ricardo Silva. Counterfactual fairness. In *Advances
576 in Neural Information Processing Systems*, volume 30. Curran Associates, Inc., 2017.
- 577
- 578 Evan Z Liu, Behzad Haghgoo, Annie S Chen, Aditi Raghunathan, Pang Wei Koh, Shiori Sagawa,
579 Percy Liang, and Chelsea Finn. Just Train Twice: Improving Group Robustness without Training
580 Group Information. In *Proceedings of the 38th International Conference on Machine Learning*,
volume 139, pp. 6781–6792, 2021.
- 581
- 582 Binh Thanh Luong, Salvatore Ruggieri, and Franco Turini. K-NN as an implementation of situation
583 testing for discrimination discovery and prevention. In *Proceedings of the 17th ACM SIGKDD
584 International Conference on Knowledge Discovery and Data Mining*, pp. 502–510. Association
585 for Computing Machinery, 2011. ISBN 978-1-4503-0813-7.
- 586
- 587 David Madras, Elliot Creager, Toniann Pitassi, and Richard Zemel. Learning Adversarially Fair and
588 Transferable Representations. In *Proceedings of the 35th International Conference on Machine
Learning*, volume 80, pp. 3384–3393. PMLR, 2018.
- 589
- 590 Gerald Marwell and Pamela Oliver. *The Critical Mass in Collective Action*. Cambridge University
591 Press, 1993.
- 592
- 593 Jeff Mattu, Julia Larson, Lauren Angwin, and Surya Kirchner. How We Analyzed the COMPAS Re-
cidivism Algorithm. [https://www.propublica.org/article/how-we-analyzed-the-compas-recidivism-
algorithm](https://www.propublica.org/article/how-we-analyzed-the-compas-recidivism-algorithm), 2016.

- 594 Doug McAdam. *Political Process and the Development of Black Insurgency, 1930-1970*. University
595 of Chicago Press, 1999.
- 596
- 597 Aditya Krishna Menon and Robert C. Williamson. The cost of fairness in binary classification. In
598 *Proceedings of the 1st Conference on Fairness, Accountability and Transparency*, pp. 107–118.
599 PMLR, 2018.
- 600 Melissa R. Michelson. Meeting the Challenge of Latino Voter Mobilization. *The ANNALS of the*
601 *American Academy of Political and Social Science*, 601(1):85–101, 2005.
- 602
- 603 Junhyun Nam, Hyuntak Cha, Sungsoo Ahn, Jaeho Lee, and Jinwoo Shin. Learning from failure:
604 De-biasing classifier from biased classifier. *Advances in Neural Information Processing Systems*,
605 33:20673–20684, 2020.
- 606 Mancur Olson. Collective action. In *The Invisible Hand*, pp. 61–69. Palgrave Macmillan UK, 1989.
607 ISBN 978-1-349-20313-0.
- 608
- 609 Geoff Pleiss, Manish Raghavan, Felix Wu, Jon Kleinberg, and Kilian Q Weinberger. On fairness and
610 calibration. In *Advances in Neural Information Processing Systems*, volume 30. Curran Associates,
611 Inc., 2017.
- 612 Bashir Sadeghi, Sepehr Dehdashtian, and Vishnu Boddeti. On Characterizing the Trade-off in
613 Invariant Representation Learning. *Transactions on Machine Learning Research*, 2022.
- 614
- 615 Shiori Sagawa, Pang Wei Koh, Tatsunori B. Hashimoto, and Percy Liang. Distributionally Robust
616 Neural Networks. In *Eighth International Conference on Learning Representations*, 2020.
- 617 Muniba Saleem, Ian Hawkins, Magdalena E. Wojcieszak, and Jessica Roden. When and how negative
618 news coverage empowers collective action in minorities. *Communication Research*, 48(2):291–316,
619 2021.
- 620
- 621 Amartya Sanyal, Yaxi Hu, and Fanny Yang. How unfair is private learning? In *Proceedings of the*
622 *Thirty-Eighth Conference on Uncertainty in Artificial Intelligence*, volume 180, pp. 1738–1748.
623 PMLR, 2022.
- 624 Dorothee Sigg, Moritz Hardt, and Celestine Mendler-Dünner. Decline now: A combinatorial model
625 for algorithmic collective action. In *Proceedings of the 2025 CHI Conference on Human Factors*
626 *in Computing Systems*. Association for Computing Machinery, 2025. ISBN 979-8-4007-1394-1.
- 627
- 628 Alexandru Tifrea, Preethi Lahoti, Ben Packer, Yoni Halpern, Ahmad Beirami, and Flavien Prost.
629 FRAPPÉ: A group fairness framework for post-processing everything. In *Proceedings of the 41st*
630 *International Conference on Machine Learning*, volume 235, pp. 48321–48343. PMLR, 2024.
- 631 Yongkai Wu, Lu Zhang, and Xintao Wu. Counterfactual fairness: Unidentification, bound and
632 algorithm. In *Proceedings of the Twenty-Eighth International Joint Conference on Artificial*
633 *Intelligence, IJCAI-19*, pp. 1438–1444. International Joint Conferences on Artificial Intelligence
634 Organization, 2019.
- 635 Richard Zemel, Yu Wu, Kevin Swersky, Toni Pitassi, and Cynthia Dwork. Learning Fair Representa-
636 tions. In *Proceedings of the 30th International Conference on Machine Learning*, volume 28, pp.
637 325–333. PMLR, 2013.
- 638
- 639 Han Zhao and Geoff Gordon. Inherent tradeoffs in learning fair representations. In *Advances in*
640 *Neural Information Processing Systems*, volume 32. Curran Associates, Inc., 2019.

642 8 APPENDIX

644 A MOTIVATING EXAMPLES

645
646
647 To recognize real-world problems that lend themselves well to collective action for fairness one needs to look for the following few characteristics:

- 648 • Firm and goal: A firm trains a predictive model primarily to minimize average error, with
649 little incentive to protect minority groups.
- 650 • End-users: People who use the platform and whose behavior generates data for the firm’s
651 dataset.
- 652 • Disadvantaged group: A subgroup of end-users who is treated unfairly.
- 653 • Relabeling possibility: How the minority can relabel themselves to make the trained classifier
654 fairer.

655
656 Here we suggest several cases that answer these characteristics.

657
658 1. Content moderation

- 659 • Firm and goal: A global social-media company optimizes a high-recall harmful-content
660 detector measured on its largest user pools.
- 661 • End-users: Everyday users of the platform who can flag offensive content.
- 662 • Disadvantaged group: Slurs, insults, or cultural references specific to minority com-
663 munities are not flagged often enough, so the model fails to detect harmful content in
664 those groups’ languages.
- 665 • Relabeling possibility: The minority flags borderline content from their community
666 that the platform’s global guidelines ignore.

667 2. Resume screening

- 668 • Firm and goal: A multi-national HR firm trains a classifier to extract skills from
669 resumes.
- 670 • End-users: Job applicants submitting resumes.
- 671 • Disadvantaged group: Applicants from a disadvantaged minority may lack formal
672 education and degrees compared to the majority, but may have informal training which
673 the classifier ignores.
- 674 • Relabeling possibility: Applicants can reframe their work experience, e.g. framing
675 working at a store as being a salesperson, or managing shifts as managerial experience.

676 3. Medical treatment prediction

- 677 • Firm and goal: A nationwide insurer builds a treatment-recommendation model to
678 minimize average costs and adverse events.
- 679 • End-users: Patients who report their treatment outcomes (pain levels, recovery time,
680 side effects).
- 681 • Disadvantaged group: Minority groups may experience different side effects or recovery
682 rates than the majority, so the model recommends suboptimal treatments for them.
- 683 • Relabeling possibility: Individual patients record more detailed outcomes rather than
684 underreporting, e.g., consistently marking “still in pain” instead of “fine”.

685 4. Credit scoring

- 686 • Firm and goal: A lender trains a credit-risk model to predict defaults and set loan terms,
687 using historical repayment data.
- 688 • End-users: Borrowers whose repayment or default becomes training labels.
- 689 • Disadvantaged group: Disadvantaged groups may not have credit cards or have never
690 taken loans, and only deal with cash but still pay their bills. These actions are “credit-
691 invisible”.
- 692 • Relabeling possibility: A borrower can report their paid bills, such as rent or utilities,
693 as repaid loans. These become additional positive repayment labels.

694 5. Recommender systems

- 695 • Firm and goal: A streaming platform trains recommender system to maximize en-
696 gagement, heavily weighted toward mainstream content Baumann & Mandler-Dünner
697 (2024).
- 698 • End-users: Users who like, skip, or re-listen to songs.
- 699 • Disadvantaged group: Niche genres or local musicians get suppressed, as engagement
700 data mostly comes from the majority’s preferences.
- 701 • Relabeling possibility: Users can promote underrepresented content by repeatedly
listening, liking, or playlisting it.

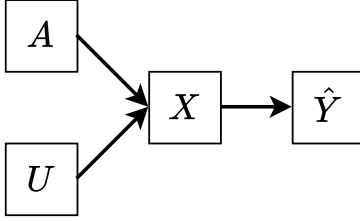


Figure 9: Assumed causal model for data generation and prediction. The group membership A and the other latent variables U are the causal parents of the observable features X . The classifier outputs a predicted label \hat{Y} that depends on the features X .

B PRELIMINARIES

B.1 STATISTICAL PARITY AND EQUALIZED ODDS

Among the various ways fairness can be defined in machine learning, group fairness is one of the most studied. Group fairness requires that a model’s predictions should not systematically differ between protected groups. One standard measure of this is statistical parity (SP), which captures the difference in the probability of a positive prediction across groups. Formally, it is defined as

$$\text{SP}(h) = |P[h(x) = 1|a = 1] - P[h(x) = 1|a = 0]|, \quad (12)$$

where a smaller SP value indicates fairer treatment across groups. However, SP does not account for the ground-truth labels y , and thus optimizing for SP can degrade the overall accuracy. For example, a classifier that always predicts $\hat{y} = 1$ will have perfect SP but a high prediction error. Alternatively, a stricter notion called equalized odds (EqOd) Hardt et al. (2016) requires that both the true positive rate and false positive rate be equal across groups. Here the EqOd difference is defined as

$$\text{EqOd}(h) = \frac{1}{2} \sum_{z=0,1} |P[h(x) = 1|a = 1, y = z] - P[h(x) = 1|a = 0, y = z]|. \quad (13)$$

B.2 SUBOPTIMAL BAYES CLASSIFIER

Definition 2 (ϵ -suboptimal classifier). *A classifier $f : \mathcal{X} \rightarrow \mathcal{Y}$ is ϵ -suboptimal on a set $\mathcal{X}' \subseteq \mathcal{X}$ under the distribution \mathbb{P} if there exists a \mathbb{P}' with $\text{TV}(\mathbb{P}_{Y|X=x}, \mathbb{P}'_{Y|X=x}) \leq \epsilon$ such that for all $x \in \mathcal{X}'$*

$$f(x) = \operatorname{argmax}_{y \in \mathcal{Y}} \mathbb{P}'(y|x).$$

$\text{TV}(\cdot, \cdot)$ is the total variation distance between two distributions. The definition is discussed more in Hardt et al. (2023).

C THEORETICAL RESULTS AND PROOFS

C.1 COUNTERFACTUAL FAIRNESS AS SUCCESS

Proposition 1. *A Bayes classifier trained on \mathbb{P}_α is minority-focused counterfactually fair if and only if the success of a minority collective is $S = 1$.*

Proof. For this proof, we assume the data is generated according to the causal model presented in Figure 9, where the features X are conditioned on the group membership A and other latent causal parent U . The features X are then used by a classifier to compute a predicted label $h(x) \hat{Y}$. In our

case, the predicted label is the output of an optimal Bayes classifier that predicts the most probable label as $h(x) = \arg \max_y P(y|x)$.

The data distribution is a mixture distribution between the majority distribution $\mathbb{P}_{A=0}$ and the minority distribution $\mathbb{P}_{A=1}$, which is defined as

$$\mathbb{P}_0 = (1 - \beta) \mathbb{P}_{A=0} + \beta \mathbb{P}_{A=1}, \quad (14)$$

where β is the proportion of the minority in the data.

The collective is employing the signal erasure strategy from Equation (4), where the erased signal is the counterfactual of x if they were a member of the majority group $A = 0$, or formally as

$$g(x) = x_{A \leftarrow 0} \sim \mathbb{P}(X_{A \leftarrow 0}). \quad (15)$$

The training distribution is a mixture distribution of the data distribution \mathbb{P}_0 and the collective distribution \mathbb{P}^* , which is defined as

$$\mathbb{P}_\alpha = \alpha \mathbb{P}^* + (1 - \alpha) \mathbb{P}_0. \quad (16)$$

We now write the success of the collective (Equation (3)) in terms of the Bayes classifier as

$$\begin{aligned} S &= \mathbb{P}_0 [h(x) = h(g(x))] \\ &= \mathbb{P}_0 \left[\arg \max_y \mathbb{P}_\alpha(y|x) = \arg \max_y \mathbb{P}_\alpha(y|g(x)) \right]. \end{aligned} \quad (17)$$

To compute this probability, we split it into two cases, conditioning on the group membership A .

When conditioning the success on the majority group $A = 0$, then $g(x) = x$ as the intervention on A , which converts to the majority, does not change the value of A , which is already the majority. This trivially leads to

$$\begin{aligned} S_{A=0} &= \mathbb{P}_0 \left[\arg \max_y \mathbb{P}_\alpha(y|x, A=0) = \arg \max_y \mathbb{P}_\alpha(y|g(x), A=0) \right] \\ &= \mathbb{P}_0 \left[\arg \max_y \mathbb{P}_\alpha(y|x, A=0) = \arg \max_y \mathbb{P}_\alpha(y|x, A=0) \right] \\ &= 1. \end{aligned} \quad (18)$$

For conditioning the success on the minority, recall that the data is generated according to the causal model in Figure 9 which means that intervention on the group membership A can be passed down to the features X as

$$\mathbb{P}(h(x_{A \leftarrow 0}) = y | X, A = 1) = \mathbb{P}(h(x) = y | X_{A \leftarrow 0}, A = 1) = \mathbb{P}(h(x) = y | g(X), A = 1). \quad (19)$$

This can be used to write the success conditioned on the minority as

$$\begin{aligned} S_{A=1} &= \mathbb{P}_0 \left[\arg \max_y \mathbb{P}_\alpha(y|x, A=1) = \arg \max_y \mathbb{P}_\alpha(y|g(x), A=1) \right] \\ &= \mathbb{P}_0 \left[\arg \max_y \mathbb{P}_\alpha(h(x_{A \leftarrow 1}) = y | X, A=1) = \arg \max_y \mathbb{P}_\alpha(h(x_{A \leftarrow 0}) = y | X, A=1) \right]. \end{aligned} \quad (20)$$

The first term is rewritten to use the intervention notation even though the intervened variable is unchanged.

As the proportion of the minority is known to be β , the success can be written by combining Equations (18) and (20) using the law of total probability as

$$\begin{aligned} S &= 1 - \beta + \beta \mathbb{P}_0 \left[\arg \max_y \mathbb{P}_\alpha(h(x_{A \leftarrow 1}) = y | X, A=1) = \arg \max_y \mathbb{P}_\alpha(h(x_{A \leftarrow 0}) = y | X, A=1) \right] \\ &= 1 - \beta \left(1 - \mathbb{P}_0 \left[\arg \max_y \mathbb{P}_\alpha(h(x_{A \leftarrow 1}) = y | X, A=1) = \arg \max_y \mathbb{P}_\alpha(h(x_{A \leftarrow 0}) = y | X, A=1) \right] \right). \end{aligned} \quad (21)$$

This equality can be examined under two scenarios: when the success is perfect $S = 1$ and when the classifier is minority-focused counterfactually fair.

810 **When the success is $S = 1$** If the success of the collective is $S = 1$, then Equation (21) leads to

811
812
$$\mathbb{P}_0 \left[\arg \max_y \mathbb{P}_\alpha (h(x_{A \leftarrow 1}) = y | X, A = 1) = \arg \max_y \mathbb{P}_\alpha (h(x_{A \leftarrow 0}) = y | X, A = 1) \right] = 1. \quad (22)$$

813
814 This means that it is certain that

815
816
$$\arg \max_y \mathbb{P}_\alpha (h(x_{A \leftarrow 1}) = y | X, A = 1) = \arg \max_y \mathbb{P}_\alpha (h(x_{A \leftarrow 0}) = y | X, A = 1), \quad (23)$$

817
818 Since the label is binary, then it follows that the same applies to using $\arg \min$. Therefore, for all
819 $y \in \{0, 1\}$ we have

820
821
$$\mathbb{P}_\alpha (h(x_{A \leftarrow 1}) = y | X, A = 1) = \mathbb{P}_\alpha (h(x_{A \leftarrow 0}) = y | X, A = 1), \quad (24)$$

822 which is the definition of a minority-focused counterfactually fair classifier (Definition 1).

823
824 **When the classifier is one-sided counterfactually fair** If the classifier is one-sided counterfactually
825 fair (Definition 1), then by definition

826
827
$$\mathbb{P}_0 \left[\arg \max_y \mathbb{P}_\alpha (h(x_{A \leftarrow 1}) = y | X, A = 1) = \arg \max_y \mathbb{P}_\alpha (h(x_{A \leftarrow 0}) = y | X, A = 1) \right] = 1 \quad (25)$$

828
829 and plugging that in Equation (21) results in $S = 1$. □

830 C.2 IMPOSSIBILITY OF FAIRNESS UNDER ERM

831
832 The following proposition follows the structure of Theorem 6 in Chaudhuri et al. (2023). For a vector
833 $x \in \mathbb{R}^d$, let $D(x)$ denote a distribution on \mathbb{R}^d with mean x . Let p and m be the number of majority
834 and minority sample, respectively with $p \gg m$.

835 **Assumption 1** (Concentration Condition, Assumption 2 from Chaudhuri et al. (2023)). *Let*
836 $x_1, \dots, x_n \stackrel{i.i.d.}{\sim} D(0)$ *in* \mathbb{R}^d . *There exist maps* $X_{\max}, c, C : \mathbb{Z}_+ \times [0, 1] \times \mathbb{Z}_+ \rightarrow \mathbb{R}$ *such that*
837 *for all* $n \geq n_0$, *all* $\delta \in (0, 1)$, *and all unit vectors* $v \in \mathbb{R}^d$, *with probability at least* $1 - \delta$

838
839
$$\max_{i \in \{1, \dots, n\}} \{v^\top x_i\} \in [X_{\max}(n, \delta, d) - c(n, \delta, d), X_{\max}(n, \delta, d) + C(n, \delta, d)]$$

840
841 and $\lim_{n \rightarrow \infty} C(n, \delta, d) = 0$, $\lim_{n \rightarrow \infty} c(n, \delta, d) = 0$.

842
843 **Data Model** Labels $y \in \{-1, 1\}$ and protected attribute $a \in \{-1, 1\}$ define four groups whose
844 class-conditional distributions share the same shape $D(\cdot)$ but have different means:

845
846
$$x | (y, a) \sim D(y\mu + ya\psi),$$

847
848 where $\mu, \psi \in \mathbb{R}^2$ and $\mu \perp \psi$, with $\hat{\mu} = \mu / \|\mu\|$ and $\hat{\psi} = \psi / \|\psi\|$. For concreteness, take $\mu =$
849 $\|\mu\| (0, 1)^\top$ and $\psi = \|\psi\| (1, 0)^\top$. Without loss of generality, let the majority attribute be $a_M = +1$
850 (the minority is $a_m = -1$). Thus the two majority means lie on the positive diagonal $\pm(\mu + \psi)$ and
851 the two minority means on the negative diagonal $\pm(\mu - \psi)$.

852 Let B, A be two sets of points that are sampled from $D(0)$. We will always associate B with
853 negatively labelled points and A with positive, as will be clear below. Following Chaudhuri et al.
854 (2023), define the sets

855
856
$$A_\mu = \{x + \mu : x \in A\}, \quad -B_\mu = \{x + \mu : x \in -B\}.$$

857 We split by attribute and (for the minority) allow arbitrary relabeling before training. Write $A_\mu^M,$
858 B_μ^M for the majority parts and A_μ^m, B_μ^m for the minority subsets used with positive/negative labels in
859 training after centering. Incorporating the attribute shifts, set

860
861
$$A_{\mu, \psi}^M = -\psi + A_\mu^M, \quad B_{\mu, \psi}^M = +\psi + B_\mu^M, \quad A_{\mu, \psi}^m = +\psi + A_\mu^m, \quad B_{\mu, \psi}^m = -\psi + B_\mu^m,$$

862 and similarly for the relabeled minority pieces $A_{\mu, \psi}^{m, \pm}$ and $B_{\mu, \psi}^{m, \pm}$ (these are subsets of $A_{\mu, \psi}^m$ and $B_{\mu, \psi}^m$,
863 respectively).

If the minority were absent, the ERM SVM converges to the spurious direction

$$w_{\text{spu}}^{\text{maj}} \propto \mu + \psi.$$

However, we assume that the minority is performing some relabeling. As a result, we denote the set $A_{\mu}^{m,+}$ as the samples relabeled with $y = 1$ and the set $A_{\mu}^{m,-}$ as the samples keeping the original label $y = 0$. Similarly we denote the set $B_{\mu}^{m,+}$ as the positive minority keeping their labels and $B_{\mu}^{m,-}$ as the positive minority who flip to $y = 0$.

Proposition 5. *Suppose $D(0)$ satisfies Assumption 1 and*

$$X_{\max}(p, \delta, 2) - X_{\max}(m, \delta, 2) \geq 2\|\psi\| + c(p, \delta, 2) + C(m, \delta, 2). \quad (26)$$

Then, for any (possibly adversarial) relabeling of minority training examples, if $p \rightarrow \infty$, with probability at least $1 - 4\delta$, the SVM ERM solution converges to the same spurious solution $w_{\text{spu}}^ \propto \mu + \psi$. Under a centrally symmetric $D(0)$ and when $\|\mu\| = \|\psi\|$, this limit satisfies EqOd (w_{spu}^*) $\rightarrow 0.5$.*

Proof. As Chaudhuri et al. (2023) shows, the ERM solution can be written as $w^* = \alpha^* \hat{\mu} + \sigma \beta^* \hat{\psi}$, where

$$\alpha^* = \arg \min_{\alpha \in [-1, 1], \sigma \in \{-1, 1\}} \sup_{x \in \{x|y=0\}} (\alpha \hat{\mu} + \sigma \beta \hat{\psi})^{\top} (x - \mu) + \sup_{x \in \{x|y=1\}} (\alpha \hat{\mu} + \sigma \beta \hat{\psi})^{\top} (x - \mu)$$

and $\beta = \sqrt{1 - \alpha^2}$.

With the shorthand

$$\begin{aligned} f_1(\alpha) &:= \sup_{x \in A_{\mu, \psi}^M} (\alpha \hat{\mu} + \sigma \beta \hat{\psi})^{\top} x, & f_{2, \pm}(\alpha) &:= \sup_{x \in A_{\mu, \psi}^{m, \pm}} (\alpha \hat{\mu} + \sigma \beta \hat{\psi})^{\top} x, \\ f_3(\alpha) &:= \sup_{x \in -B_{\mu, \psi}^M} (\alpha \hat{\mu} + \sigma \beta \hat{\psi})^{\top} x, & f_{4, \pm}(\alpha) &:= \sup_{x \in -B_{\mu, \psi}^{m, \pm}} (\alpha \hat{\mu} + \sigma \beta \hat{\psi})^{\top} x, \end{aligned}$$

the SVM objective is

$$\begin{aligned} F(\alpha) = \min_{\alpha} \left\{ \max \left(f_1(\alpha) - \alpha \|\mu\| + \sigma \beta \|\psi\|, \right. \right. \\ f(\alpha) - \alpha \|\mu\| - \sigma \beta \|\psi\|, \\ f_{4,-}(\alpha) - \alpha \|\mu\| - \sigma \beta \|\psi\| \\ \left. \left. + \max \left(f_3(\alpha) - \alpha \|\mu\| + \sigma \beta \|\psi\|, \right. \right. \right. \\ f_{2,+}(\alpha) - \alpha \|\mu\| - \sigma \beta \|\psi\|, \\ \left. \left. \left. f_{4,+}(\alpha) - \alpha \|\mu\| - \sigma \beta \|\psi\| \right) \right\}. \end{aligned}$$

By Assumption 1, for the majority group of size p , there exists X_p, c_p, C_p such that, with probability at least $1 - 4\delta$ and for all α ,

$$f_1(\alpha), f_3(\alpha) \in [X_p - c_p, X_p + C_p]. \quad (27)$$

For any minority relabeling, $A_{\mu, \psi}^{m, \pm} \subseteq A_{\mu, \psi}^M$ and $-B_{\mu, \psi}^{m, \pm} \subseteq -B_{\mu, \psi}^M$, so the same assumption gives

$$f_{2, \pm}(\alpha), f_{4, \pm}(\alpha) \leq X_m + C_m, \quad (28)$$

where $X_m := X_{\max}(m, \delta, 2)$ and $C_m := C(m, \delta, 2)$. Using Equation (26), we get

$$X_p - X_m \geq 2\|\psi\| + c_p + C_m. \quad (29)$$

Combining Equations (27) to (29), still uniformly in α , we obtain

$$\begin{aligned} f_1(\alpha) - f_{2, \pm}(\alpha) &\geq 2\|\psi\|, & f_1(\alpha) - f_{4, \pm}(\alpha) &\geq 2\|\psi\|, \\ f_3(\alpha) - f_{2, \pm}(\alpha) &\geq 2\|\psi\|, & f_3(\alpha) - f_{4, \pm}(\alpha) &\geq 2\|\psi\|. \end{aligned} \quad (30)$$

918 **Case 1:** $\sigma = 1$. Consider the *first* inner maximum inside $F(\alpha)$. Compare the majority entry
 919 (associated with $f_1(\alpha)$) to the minority entries ($f_{2,-}(\alpha), f_{4,-}(\alpha)$):
 920

$$\begin{aligned} 921 \quad [f_1(\alpha) - \alpha \|\mu\| + \beta \|\psi\|] - [f_{2,-}(\alpha) - \alpha \|\mu\| - \beta \|\psi\|] &= (f_1(\alpha) - f_{2,-}(\alpha)) + 2\beta \|\psi\| \\ 922 &\geq 2 \|\psi\| + 2\beta \|\psi\| \\ 923 &\geq 0 \end{aligned}$$

924 and similarly against $f_{4,-}$. Hence the first maximum equals $f_1 - \alpha \|\mu\| + \beta \|\psi\|$. For the *second*
 925 inner maximum, the same comparison yields the majority term $f_3 - \alpha \|\mu\| + \beta \|\psi\|$. Summing then
 926 for $\sigma = 1$ we have,
 927

$$928 \quad F_+(\alpha) = f_1(\alpha) + f_3(\alpha) - 2\alpha \|\mu\| + 2\beta \|\psi\|.$$

929 **Case 2:** $\sigma = -1$. For the first inner max in $F(\alpha)$,

$$\begin{aligned} 930 \quad [f_1(\alpha) - \alpha \|\mu\| - \beta \|\psi\|] - [f_{2,-}(\alpha) - \alpha \|\mu\| + \beta \|\psi\|] &= (f_1(\alpha) - f_{2,-}(\alpha)) - 2\beta \|\psi\| \\ 931 &\geq 2 \|\psi\| - 2\beta \|\psi\| \\ 932 &\geq 0 \end{aligned}$$

933 and likewise against $f_{4,-}$. Thus the first maximum equals $f_1 - \alpha \|\mu\| - \beta \|\psi\|$. The second inner max
 934 is analogous and equals $f_3 - \alpha \|\mu\| - \beta \|\psi\|$. Therefore,
 935

$$936 \quad F_-(\alpha) = f_1(\alpha) + f_3(\alpha) - 2\alpha \|\mu\| - 2\beta \|\psi\|.$$

937 For every α , $F_+(\alpha) = (f_1 + f_3) - 2\alpha \|\mu\| + 2\beta \|\psi\|$ and $F_-(\alpha) = (f_1 + f_3) - 2\alpha \|\mu\| - 2\beta \|\psi\|$,
 938 so $F_+(\alpha) \geq F_-(\alpha)$. Hence the optimal sign is $\sigma = -1$ and the objective reduces to
 939

$$940 \quad F(\alpha) = (f_1(\alpha) + f_3(\alpha)) - 2\alpha \|\mu\| - 2\beta \|\psi\|.$$

941 Maximizing $\alpha \|\mu\| + \beta \|\psi\|$ is equivalent to minimizing $F(\alpha)$ up to the bounded change (due to As-
 942 sumption 1) of $f_1(\alpha) + f_3(\alpha)$. Next, we use the following lemma.
 943

944 **Lemma 1** (Approximate Maximization Lemma - I, Lemma 14 from Chaudhuri et al. (2023)). *Let*
 945 $F(\alpha) = f(\alpha) + g(\alpha)$ *where* $g(\alpha) = \alpha u + \sqrt{1 - \alpha^2} v$, $u, v > 0$, *and* $f(\alpha) \in [-L, U]$. *Let*
 946 $\alpha_F \in \operatorname{argmax}_\alpha F(\alpha)$, *and let* $\alpha_g = \frac{u}{\sqrt{u^2 + v^2}} \in \operatorname{argmax}_\alpha g(\alpha)$.
 947

948 *Then, the angle between* $(\alpha_F, \sqrt{1 - \alpha_F^2})$ *and* $(\alpha_g, \sqrt{1 - \alpha_g^2})$ *is at most* $\cos^{-1} \left(1 - \frac{L+U}{\sqrt{u^2 + v^2}} \right)$, *and*
 949 $\max_\alpha F(\alpha) \geq \sqrt{u^2 + v^2} - L$.
 950

951 Applying Lemma 1 with $u = \|\mu\|$ and $v = \|\psi\|$ shows that (α, β) approaches
 952

$$953 \quad (\alpha_g, \beta_g) = \left(\frac{\|\mu\|}{\sqrt{\|\mu\|^2 + \|\psi\|^2}}, \frac{\|\psi\|}{\sqrt{\|\mu\|^2 + \|\psi\|^2}} \right)$$

954 as $p \rightarrow \infty$. Thus
 955

$$956 \quad w^* \longrightarrow w_{\text{spu}}^* = \alpha_g \hat{\mu} + \beta_g \hat{\psi},$$

957 independently of how the minority samples were relabeled in training.
 958

959 Under a centrally symmetric $D(0)$ and if $\|\mu\| = \|\psi\|$, the majority group ($a = +1$) separates perfectly
 960 in the limit, while the minority group ($a = -1$) has symmetric measure about the threshold, giving
 961 $\text{TPR}_{a=+1} \rightarrow 1$, $\text{FPR}_{a=+1} \rightarrow 0$, and $\text{TPR}_{a=-1} = \text{FPR}_{a=-1} \rightarrow \frac{1}{2}$. Hence $\text{EqOd}(w_{\text{spu}}^*) \rightarrow 0.5$.
 962

963 \square

964 This result can also be extended to \mathbb{R}^d using techniques similar to those in Chaudhuri et al. (2023).
 965 This result also encompasses the 4-Gaussian mixture model $\mathbb{P}_{4\text{GMM}}$ used in Section 5 as a special
 966 case, leading to the following.
 967

968 **Proposition 2** (Informal). *Consider the dataset* $\mathbb{P}_{4\text{GMM}}$, *where every minority point participates in*
 969 *the ACA by flipping all* $y = 0$ *labels to* $y = 1$. *Then, under sufficiently separable clusters, with high*
 970 *probability, the EqOd of the ERM classifier minimizing the logistic loss will asymptotically approach*
 971 0.5 .

972 C.3 SUCCESS BOUND WITH LABEL ERROR

973 The following proof uses Lemma 11 from Hardt et al. (2023).

974 **Lemma 2** (Lemma 11 from Hardt et al. (2023)). *Suppose that P, P' are two distributions such that*
 975 *$\text{TV}(P, P') \leq \epsilon$. Take any two events E_1, E_2 measurable under P, P' . If $P(E_1) > P(E_2) + \frac{\epsilon}{1-\epsilon}$,*
 976 *then $P'(E_1) > P'(E_2)$.*

977 **Proposition 3.** *With algorithm $\mathcal{A}(x)$ with label error ρ , the success of the collective is bounded by*

$$978 S(\alpha) \geq 1 - \frac{2(1-\alpha)}{(1-2\rho)\alpha} \tau - \frac{\epsilon}{(1-\epsilon)(1-2\rho)\alpha}. \quad (11)$$

979 *Proof.* This proof follows closely the proof of Theorem 5 by Hardt et al. (2023). We start under the
 980 assumption of an optimal Bayes classifier, setting $\epsilon = 0$.

981 When the new label y' is wrong with probability ρ , then we can think of the collective as being union
 982 of two sub-collectives: one with the correct label and one with the incorrect label. In the binary case
 983 this can be formulated with correct subcollective P^+ as having label $y' = \arg \max_y P_0(y|g(x))$ and
 984 the incorrect subcollective P^- as with label $y' = \arg \min_y P_0(y|g(x))$. Then we can write the train
 985 distribution as

$$986 P_\alpha = \alpha(\rho P^- + (1-\rho)P^+) + (1-\alpha)P_0 \quad (31)$$

$$987 = \alpha\rho P^- + (1-\rho)\alpha P^+ + (1-\alpha)P_0.$$

988 Denote $y^*(x) = \arg \max_y P_0(y|g(x))$, then the probability to get prediction y^* is

$$989 P_\alpha(y^*|x) = \alpha\rho P^-(y^*|x) + (1-\rho)\alpha P^+(y^*|x) + (1-\alpha)P_0(y^*|x) \quad (32)$$

$$990 = (1-\rho)\alpha + (1-\alpha)P_0(y^*|x),$$

991 and the probability to get the prediction $y \neq y^*$ is

$$992 P_\alpha(y|x) = \alpha\rho P^-(y|x) + (1-\rho)\alpha P^+(y|x) + (1-\alpha)P_0(y|x) \quad (33)$$

$$993 = \alpha\rho + (1-\alpha)P_0(y|x),$$

994 where $P^+(y^*|x) = 1, P^-(y^*|x) = 0, P^+(y \neq y^*|x) = 0, P^-(y \neq y^*|x) = 1$ by definition.

995 A Bayes classifier h returns the most probable label $h(x) = \arg \max_y P(y|x)$. Therefore, a Bayes
 996 classifier will output y^* if the probability is greater, which can be written as the condition

$$1000 P_\alpha(y^*|x) > P_\alpha(y|x)$$

$$1001 (1-\rho)\alpha + (1-\alpha)P_0(y^*|x) > \alpha\rho + (1-\alpha)P_0(y|x) \quad (34)$$

$$1002 (1-2\rho)\alpha > (1-\alpha)(P_0(y|x) - P_0(y^*|x)).$$

1003 Let $\tau(x) = \max_y [P_0(y|x) - P_0(y|g(x))]$, then

$$1004 P_0(y|x) - P_0(y^*|x) \leq P_0(y|x) - P_0(y|g(x)) + P_0(y^*|g(x)) - P_0(y^*|x) \quad (35)$$

$$1005 \leq 2\tau(x).$$

1006 With that, the condition in Equation (34) can be written as

$$1007 (1-2\rho)\alpha > 2(1-\alpha)\tau(x). \quad (36)$$

1008 With that, the success can be bounded as

$$1009 S = P_0[f(x) = f(g(x))]$$

$$1010 = P_0[f(x) = y^*(x)]$$

$$1011 \geq P_0[(1-2\rho)\alpha > 2(1-\alpha)\tau(x)]$$

$$1012 = P_0\left[1 - \frac{2(1-\alpha)}{(1-2\rho)\alpha}\tau(x) > 0\right]$$

$$1013 = \mathbb{E}_{x \sim P_0}\left[\mathbf{1}\left\{1 - \frac{2(1-\alpha)}{(1-2\rho)\alpha}\tau(x) > 0\right\}\right] \quad (37)$$

$$1014 \geq \mathbb{E}_{x \sim P_0}\left[1 - \frac{2(1-\alpha)}{(1-2\rho)\alpha}\tau(x)\right]$$

$$1015 = 1 - \frac{2(1-\alpha)}{(1-2\rho)\alpha}\tau$$

1026 **With sub-optimality** $\epsilon > 0$ A result of Lemma 2 is to write the condition in Equation (36) as

$$1027 \quad (1 - 2\rho)\alpha > 2(1 - \alpha)\tau(x) + \frac{\epsilon}{1 - \epsilon}, \quad (38)$$

1028 which by following the same steps as with $\epsilon = 0$ results in the final bound

$$1029 \quad S(\alpha) \geq 1 - \frac{2(1 - \alpha)}{(1 - 2\rho)\alpha}\tau - \frac{\epsilon}{(1 - \epsilon)(1 - 2\rho)\alpha}. \quad (39)$$

1030 \square

1031 C.4 LABEL ERROR WITH BETTER REPRESENTATION

1032 For the following we assume a similar setting as in Appendix C.2, visualised as a 2D distribution
1033 in Figure 6. We are given the majority data, and tasked with labeling the minority data. Assume
1034 all labels are distributed equally $\mathbb{P}[Y = 1] = \mathbb{P}[Y = -1] = \frac{1}{2}$. The minority features X_{\min} are
1035 distributed as $X_{\min} \sim \mathcal{N}(y\mu_{\min}, \Sigma_{\min})$ with $X_{\min} \in \mathbb{R}^d$. The label $\hat{y}_{\text{INN}}^{(n)}$ is predicted according to
1036 a 1NN classifier from n majority samples $\mathcal{D}_n = (x_i, y_i)_{i=0}^n$. Majority samples with $y = +1$ are
1037 distributed as $X_+ \sim \mathcal{N}(\mu, \Sigma)$, and with $y = -1$ are distributed as $X_- \sim \mathcal{N}(-\mu, \Sigma)$.

1038 **Theorem 1.** Assume that $\mu_{\min}^\top \Sigma^{-1} \mu > 0$. Further, consider the setting with $\Sigma_{\min} = I$, and the
1039 minority (i.e. test) distribution introduced above with $\mathbb{P}[Y = 1] = \mathbb{P}[Y = -1] = 0.5$ and $X_{\min} \sim$
1040 $\mathcal{N}(y\mu_{\min}, \Sigma_{\min})$.

1041 Then, there exists a projection $P \in \mathbb{R}^{d \times d}$ such that asymptotically for $n \rightarrow \infty$, $\text{err}_{\text{INN}}^{\text{rep}} < \text{err}_{\text{INN}}^{\text{raw}}$.

1042 *Proof.* Consider the projection on the hyperplane perpendicular to w , where $w = \frac{\mu - \mu_{\min}}{2}$. The
1043 projection matrix associated with this transformation is $P = I - \frac{ww^\top}{w^\top w}$.

1044 Let us denote the symbols after the projection as $\bar{\mu} := P\mu$, $\bar{\mu}_{\min} := P\mu_{\min}$, $\bar{v} := (P\Sigma P^\top)^+ \bar{\mu}$ and
1045 $\bar{\Sigma}_{\min} := P\Sigma_{\min}P^\top$. Here we denoted using A^+ the pseudoinverse of the matrix A . Note that since P
1046 is an orthogonal projection matrix, it holds that $PP = P$ and $P^\top = P$.

1047 We apply Lemma 3 to obtain closed forms for the asymptotic error of 1NN applied to the initial
1048 representation and to the features after the projection P . Namely, using the notation $v := \Sigma^{-1}\mu$ we
1049 have:

$$1050 \quad \text{err}_{\text{INN}} = \frac{1}{2}\mathbb{P}_{X_{\min}|y=1}[\hat{y}_{\text{INN}} = -1] + \frac{1}{2}\mathbb{P}_{X_{\min}|y=-1}[\hat{y}_{\text{INN}} = 1] \quad (40)$$

$$1051 \quad = \frac{1}{2} \left(1 - \Phi \left(\frac{v^\top \mu_{\min}}{\sqrt{v^\top \Sigma_{\min} v}} \right) \right) + \frac{1}{2} \Phi \left(\frac{-v^\top \mu_{\min}}{\sqrt{v^\top \Sigma_{\min} v}} \right) \quad (41)$$

$$1052 \quad = 1 - \Phi \left(\frac{v^\top \mu_{\min}}{\sqrt{v^\top \Sigma_{\min} v}} \right) \quad (42)$$

$$1053 \quad = 1 - \Phi(\text{SNR}), \quad (43)$$

1054 where we used the fact that $\Phi(-z) = 1 - \Phi(z)$ and we denote $\text{SNR} := \frac{v^\top \mu_{\min}}{\sqrt{v^\top \Sigma_{\min} v}}$.

1055 Similarly, let us denote the SNR corresponding to 1NN applied on the projected representation as
1056 follows: $\text{SNR}_{\text{proj}} := \frac{\bar{v}^\top \bar{\mu}_{\min}}{\sqrt{\bar{v}^\top \bar{\Sigma}_{\min} \bar{v}}}$.

1057 To show that $\text{err}_{\text{INN}} > \text{err}_{\text{INN}}^{\text{rep}}$ it suffices to prove that $\text{SNR} < \text{SNR}_{\text{proj}}$.

1058 We begin by rewriting the numerator of SNR_{proj} . Since $\mu \in \text{Im}(P)$ and because on $\text{Im}(P)$ the
1059 operators Σ^{-1} and $(P\Sigma P^\top)^+$ represent the same transformation, it follows that:

$$1060 \quad \bar{v} = (P\Sigma P^\top)^+ \bar{\mu} = \Sigma^{-1} \bar{\mu}.$$

Moving on the the denominator of SNR_{proj} , we have that:

$$\begin{aligned}
\bar{v}^\top \bar{\Sigma}_{\min} \bar{v} &= \bar{v}^\top (P \Sigma_{\min} P^\top)^+ \bar{v} \\
&= \bar{v}^\top (PP^\top)^+ \bar{v} \\
&= \bar{v}^\top P^+ \bar{v} \\
&= \bar{v}^\top P \bar{v} \\
&= \bar{v}^\top \bar{v} \\
&= \|\bar{v}\|^2.
\end{aligned}$$

In the second line we used the fact that $\Sigma_{\min} = I$, in the third line we use the identity $P^2 = P$ due to P being a projection matrix, in the fourth line we use $P^+ = P$ since P is an orthogonal projection (i.e. P is symmetric) and in the fifth line we use the fact that $\bar{v} \in \text{Im}(P)$, and hence, $P\bar{v} = \bar{v}$.

Putting everything together, and using the fact that Σ (and thus, Σ^{-1}) is positive definite (i.e. $x^\top \Sigma^{-1} x > 0, \forall x \in \mathbb{R}^d$) we get that:

$$SNR_{\text{proj}} = \frac{\bar{\mu}^\top \Sigma^{-1} \bar{\mu}}{\|\bar{v}\|^2} > 0 > \frac{\mu^\top \Sigma^{-1} \mu_{\min}}{\|\Sigma^{-1} \mu\|^2} = SNR.$$

□

Lemma 3. For a unimodal minority distribution $X_{\min} \sim \mathcal{N}(\mu_{\min}, \Sigma_{\min})$ it holds that:

$$\lim_{n \rightarrow \infty} \mathbb{P}_{X_{\min}}[\hat{y}_{\text{INN}}^{(n)} = -1] = 1 - \Phi\left(\frac{v^\top \mu_{\min}}{\sqrt{v^\top \Sigma_{\min} v}}\right),$$

where $v := \mu^\top \Sigma^{-1}$ and Φ is the CDF of a standard Gaussian.

Proof. Let us denote $\hat{y}_{\text{INN}} := \lim_{n \rightarrow \infty} \hat{y}_{\text{INN}}^{(n)}$ and let p_+ and p_- be the densities of two class-conditional distribution. Notice that the two class conditional training distributions are supported on the entire domain of \mathbb{R}^d . Therefore, in the asymptotic regime, the label \hat{y}_{INN} at a test point x is given according to the class-conditional distribution that has higher density. Namely, we have:

$$\hat{y}_{\text{INN}} = \begin{cases} -1 & \text{if } p_+(x) < p_-(x), \\ 1 & \text{otherwise.} \end{cases}$$

Given $X_{\min} \sim \mathcal{N}(\mu_{\min}, \Sigma_{\min})$, we can then write the probability of predicting $\hat{y}_{\text{INN}} = -1$ as:

$$\mathbb{P}_{X_{\min}}[\hat{y}_{\text{INN}} = -1] = \mathbb{P}_{X_{\min}}[p_+(x) < p_-(x)].$$

Using the closed forms for the pdf of a Gaussian, we write the corresponding log-probabilities as follows:

$$\log p_+(x) = -\frac{1}{2}(x - \mu)^\top \Sigma^{-1}(x - \mu) + \text{const.}$$

$$\log p_-(x) = -\frac{1}{2}(x + \mu)^\top \Sigma^{-1}(x + \mu) + \text{const.}$$

Using the fact that log is monotonically increasing and Σ (and by extension Σ^{-1}) is a symmetric matrix, we can write after some simple calculations:

$$\mathbb{P}_{X_{\min}}[\hat{y}_{\text{INN}} = -1] = \mathbb{P}_{X_{\min}}[\mu^\top \Sigma^{-1} x < 0].$$

Let us denote the random variable $Z := (\mu^\top \Sigma^{-1})X$. Since Z is a linear transformation of Gaussian random variable, it is itself Gaussian and we can write its mean and variance as follows:

$$\mu_Z := v^\top \mu_{\min}, \text{ and } \sigma_Z^2 := v^\top \Sigma_{\min} v, \text{ where } v := \mu^\top \Sigma^{-1}.$$

After this change of variable, we can rewrite the probability of predicting $\hat{y}_{1\text{NN}} = -1$ as:

$$\begin{aligned} \mathbb{P}_{X_{\min}}[\hat{y}_{1\text{NN}} = -1] &= \mathbb{P}_Z[Z < 0] \\ &= \Phi\left(\frac{0 - \mathbb{E}[Z]}{\sqrt{\text{Var}[Z]}}\right) \\ &= \Phi\left(\frac{-(\mu^\top \Sigma^{-1})^\top \mu_{\min}}{\sqrt{(\mu^\top \Sigma^{-1})^\top \Sigma_{\min} (\mu^\top \Sigma^{-1})}}\right) \\ &= 1 - \Phi\left(\frac{(\mu^\top \Sigma^{-1})^\top \mu_{\min}}{\sqrt{(\mu^\top \Sigma^{-1})^\top \Sigma_{\min} (\mu^\top \Sigma^{-1})}}\right). \end{aligned}$$

□

Note that the error from Theorem 1 is defined the same as ρ (Equation (10)). This leads to the following.

Proposition 4 (Informal). *Let data be drawn from $\mathbb{P}_{4\text{GMM}}$, and ρ_{plain} denote the error of a 1-NN classifier that assigns the label of the nearest majority neighbor in the original feature space. Then there exists a fair representation in which a 1-NN classifier achieves error ρ_{FRL} such that, asymptotically with respect to the dataset size, $\rho_{\text{FRL}} \leq \rho_{\text{plain}}$.*

D TECHNICAL DETAILS

D.1 DATASETS

COMPAS The Correctional Offender Management Profiling for Alternative Sanctions (COMPAS) dataset contains the data of criminal defendants in Broward county sheriff’s office in Florida with the task of predicting the recidivism risk. The label in this dataset represents whether the person re-offended and the sensitive attribute is the race. We follow the same data cleaning and pre-processing as Alghamdi et al. (2022).

Adult The Adult dataset Becker & Kohavi (1996) contains demographic features of US citizens and is tasked with predicting the income level of an individual. The label represents if the individual has income higher than \$50,000 and the sensitive attribute we use is the race. We follow the same data cleaning and pre-processing as Alghamdi et al. (2022).

HSLs The High School Longitudinal Study of 2009 (HSLs) Jeong et al. (2022) contains details of high-school students across the US and the task is to predict the academic success of the students. The label represents the exam score and the sensitive attribute is the race. We follow the same data cleaning and pre-processing as Alghamdi et al. (2022).

ACS-Income Ding et al. (2021) offer different classification tasks derived by US census data. In our work we used the pre-defined task of predicting level of income denoted as *ACSIncome*, where the data is already pre-processed. The label represents if the individual has income higher than \$50,000 and the sensitive attribute is the race.

Waterbirds The waterbirds dataset Sagawa et al. (2020) contains images of landbirds and waterbirds super-imposed on either land or water backgrounds, with the task of classifying the image as of a landbird or a waterbird. The label represents the type of bird, and the sensitive attribute is whether the background is land or water. To obtain the features, we used the output of the penultimate layer of a pre-trained ResNet-18 network from *PyTorch*¹. We report the results on those features

¹<https://pytorch.org/vision/main/models/generated/torchvision.models.resnet18.html>

1188 as Waterbirds-Full. We also performed PCA (using *scikit-learn*) and kept the first 85 principal
 1189 components which retain about 75% of the variance, and report the results of these components as
 1190 Waterbirds-PCA.

1191
 1192 **CivilComments** The CivilComments dataset Borkan et al. (2019) is a collection of text comments
 1193 found on the internet, with the goal of training a classifier to fairly detect toxicity. For this paper,
 1194 we modified the dataset to keep only the comments that include either *christian* or *muslim* (but not
 1195 both), with a label 0 meaning toxic and 1 meaning safe. To obtain the features, we used the word
 1196 embeddings given by Hugging Face’s *bert-base-uncased* model². We report the results on those
 1197 features as CivilComments-Full. We also performed PCA (using *scikit-learn*) and kept the first
 1198 100 principal components which retain about 75% of the variance, and report the results of these
 1199 components as CivilComments-PCA.

1200 D.2 TRAINING

1201
 1202 All classification experiments were trained with *scikit-learn*’s histogram-based gradient boosting
 1203 classification tree with the default parameters³. When there was not a pre-defined test set, we set the
 1204 train-test split as 80-20 before applying the collective action.

1205 The probabilities for RB-prob were inferred by training *scikit-learn*’s histogram-based gradient boost-
 1206 ing classification tree on the majority data with the default parameters, and using its *predict_proba*
 1207 function. For LFR Zemel et al. (2013) we used the implementation in *Holistic AI*’s open source
 1208 library⁴ with the default parameters. For FARE Jovanović et al. (2023) we used the official imple-
 1209 mentation⁵ with hyperparameters $\gamma = 0.85$, $k = 200$ and $n = 100$. For all distance computation we
 1210 used the Euclidean norm ℓ^2 -norm as $d(v, u) = \|v - u\|_2 = \sqrt{\sum_i (v_i - u_i)^2}$.

1211 E ADDITIONAL RESULTS

1212 E.1 COMPARISON WITH PRIOR WORK

1213
 1214 We compare our method RB-prob with the existing methods KDP Luong et al. (2011) and CND Kami-
 1215 ran & Calders (2009) in Figure 10. Note than CND requires flipping labels for both majority and
 1216 minority members, and we report the total number of label flips. Figure 10 shows that our method,
 1217 motivated by the counterfactual labeling, is more efficient in terms of required number of label flips,
 1218 than the existing works.

1219 E.2 EXPANDED RESULTS

1220
 1221 The following figures include the results of the experiments reported in the main text using all methods
 1222 on all dataset, both with EqOd (Equation (2)) and SP (Equation (12)) as a measure of unfairness

1238
 1239 ²<https://huggingface.co/google-bert/bert-base-uncased>

1240 ³scikit-learn.org/stable/modules/generated/sklearn.ensemble.HistGradientBoostingClassifier.html

1241 ⁴<https://github.com/holistic-ai/holisticai>

⁵<https://github.com/eth-sri/fare>

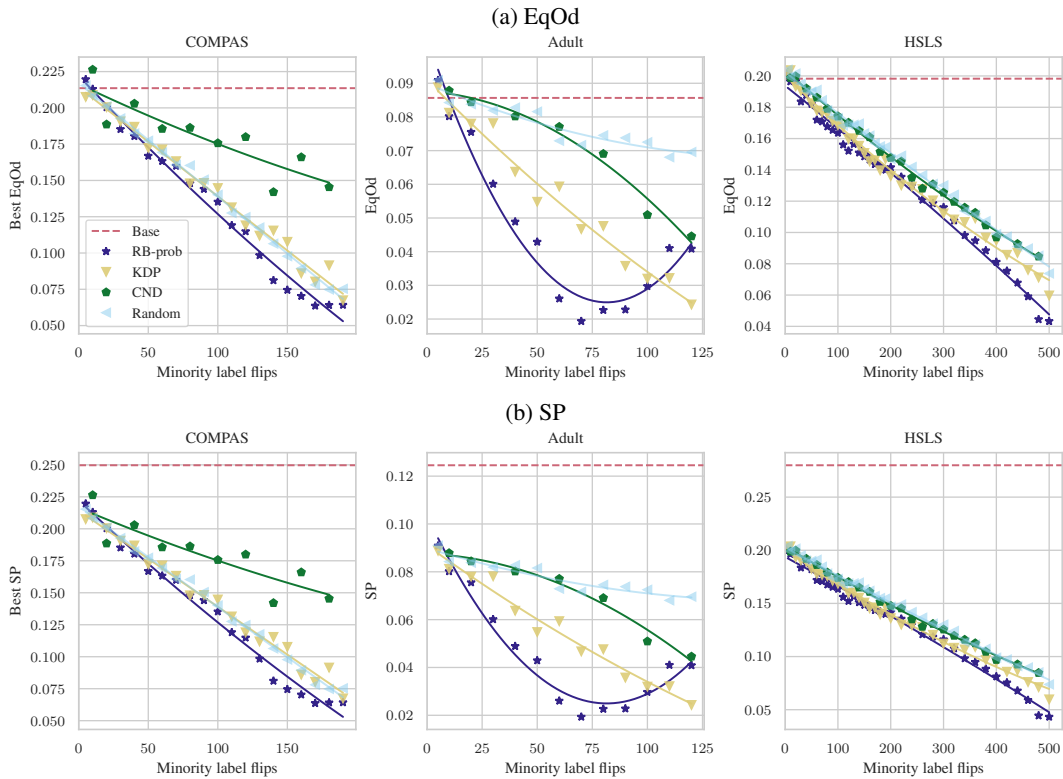


Figure 10: Fairness per number of label flips of the Random baseline, our method RB-prob, and the existing methods KDP (Luong et al., 2011) and CND (Kamiran & Calders, 2009). Our method is more efficient than prior work, requiring less flips to achieve the same level of fairness. Note that in this experiment CND could flip any label, while all other methods were restricted to the labels of 30% of the minority.

1296
1297
1298
1299
1300
1301
1302
1303
1304
1305
1306
1307
1308
1309
1310
1311
1312
1313
1314
1315
1316
1317
1318
1319
1320
1321
1322
1323
1324
1325
1326
1327
1328
1329
1330
1331
1332
1333
1334
1335
1336
1337
1338
1339
1340
1341
1342
1343
1344
1345
1346
1347
1348
1349

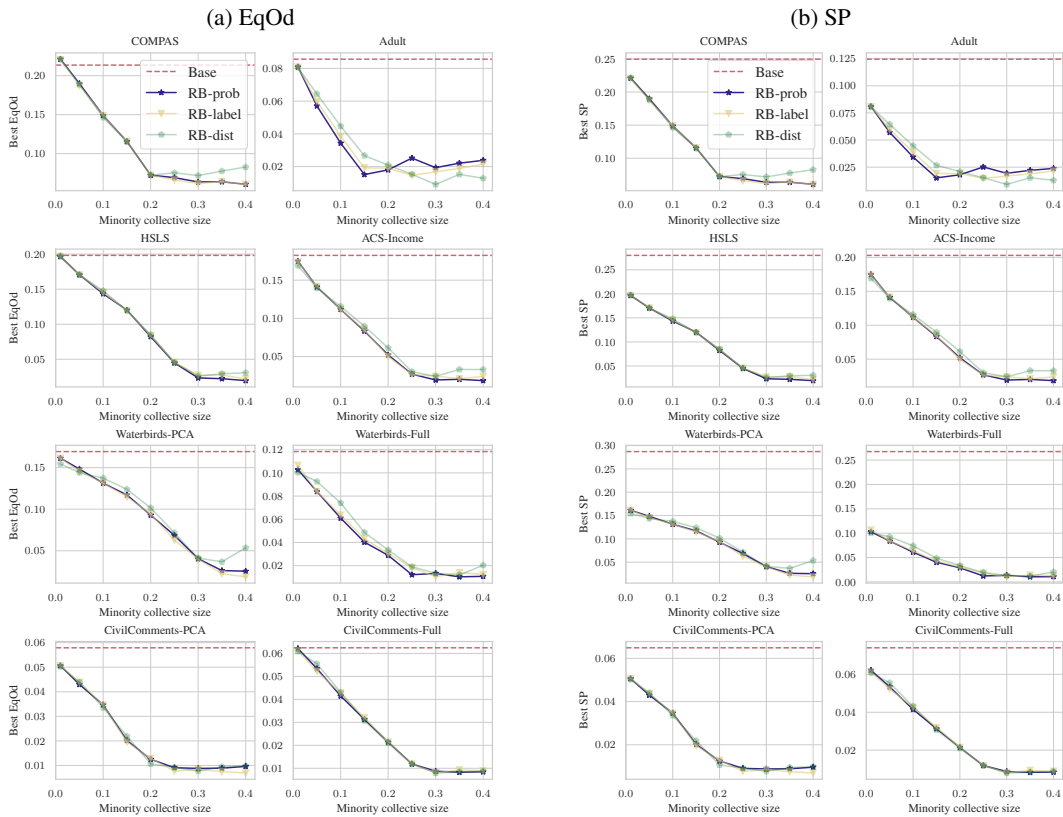


Figure 11: The lowest EqOd violation a collective can achieve greatly improves as the collective size increases, up to a certain point. Each point is a mean of 10 runs, with the standard deviation being smaller than the markers. In all the datasets we experimented on, the lowest EqOd converges around $\alpha = 0.3$.

1350
 1351
 1352
 1353
 1354
 1355
 1356
 1357
 1358
 1359
 1360
 1361
 1362
 1363
 1364
 1365
 1366
 1367
 1368
 1369
 1370
 1371
 1372
 1373
 1374
 1375
 1376
 1377
 1378
 1379
 1380
 1381
 1382
 1383
 1384
 1385
 1386
 1387
 1388
 1389
 1390
 1391
 1392
 1393
 1394
 1395
 1396
 1397
 1398
 1399
 1400
 1401
 1402
 1403

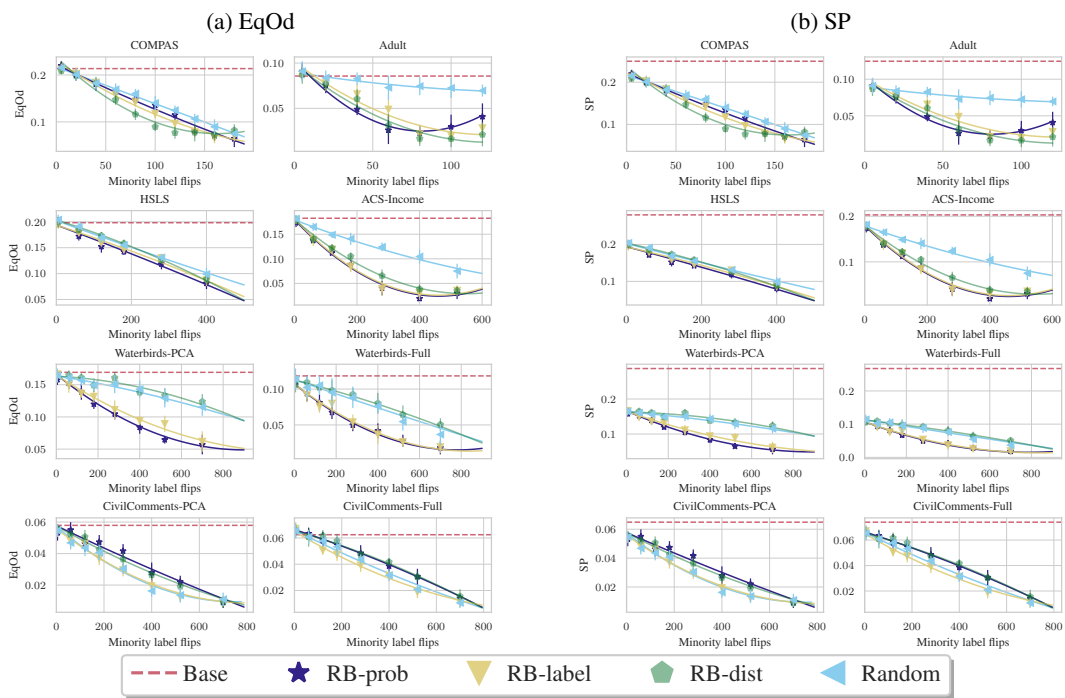


Figure 12: Our proposed methods are consistently more efficient than randomly flipping labels, requiring less label flips to attain the same level of EqOd. Each marker is the mean of 10 random runs with a specific number of label flips. The dashed line shows the mean EqOd for a classifier trained on the dataset without collective action.

1404
 1405
 1406
 1407
 1408
 1409
 1410
 1411
 1412
 1413
 1414
 1415
 1416
 1417
 1418
 1419
 1420
 1421
 1422
 1423
 1424
 1425
 1426
 1427
 1428
 1429
 1430
 1431
 1432
 1433
 1434
 1435
 1436
 1437
 1438
 1439
 1440
 1441
 1442
 1443
 1444
 1445
 1446
 1447
 1448
 1449
 1450
 1451
 1452
 1453
 1454
 1455
 1456
 1457

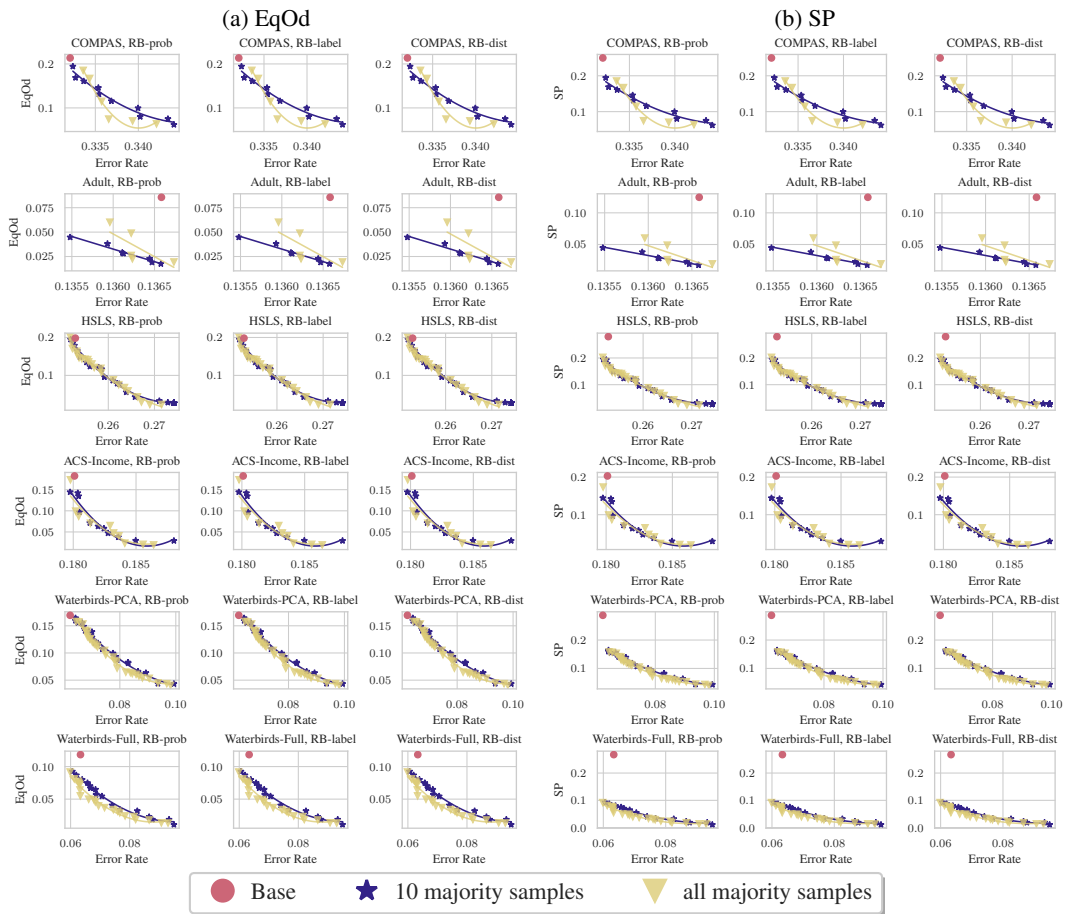


Figure 13: Limiting the knowledge of the collective about the majority does not significantly harm the Pareto front. Each point is the mean of 10 runs and the curves are fitted to guide the eye.

1458
 1459
 1460
 1461
 1462
 1463
 1464
 1465
 1466
 1467
 1468
 1469
 1470
 1471
 1472
 1473
 1474
 1475
 1476
 1477
 1478
 1479
 1480
 1481
 1482
 1483
 1484
 1485
 1486
 1487
 1488
 1489
 1490
 1491
 1492
 1493
 1494
 1495
 1496
 1497
 1498
 1499
 1500
 1501
 1502
 1503
 1504
 1505
 1506
 1507
 1508
 1509
 1510
 1511

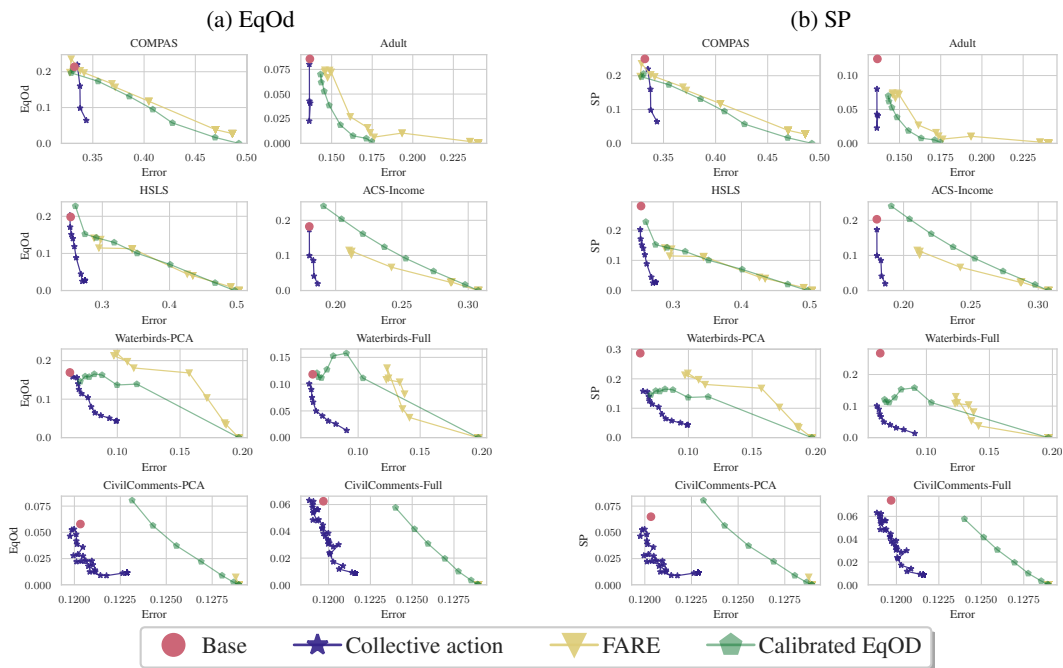


Figure 14: The firm-side pre-processing method FARE Jovanović et al. (2023) and the post-processing method calibrated equalized odds Pleiss et al. (2017) attain 0 EqOd with large error, while RB-prob with $\alpha = 0.3$ (Section 3) has much smaller error and less unfairness than the base classifier, but unable to get 0 EqOd.

1512
 1513
 1514
 1515
 1516
 1517
 1518
 1519
 1520
 1521
 1522
 1523
 1524
 1525
 1526
 1527
 1528
 1529
 1530
 1531
 1532
 1533
 1534
 1535
 1536
 1537
 1538
 1539
 1540
 1541
 1542
 1543
 1544
 1545
 1546
 1547
 1548
 1549
 1550
 1551
 1552
 1553
 1554
 1555
 1556
 1557
 1558
 1559
 1560
 1561
 1562
 1563
 1564
 1565

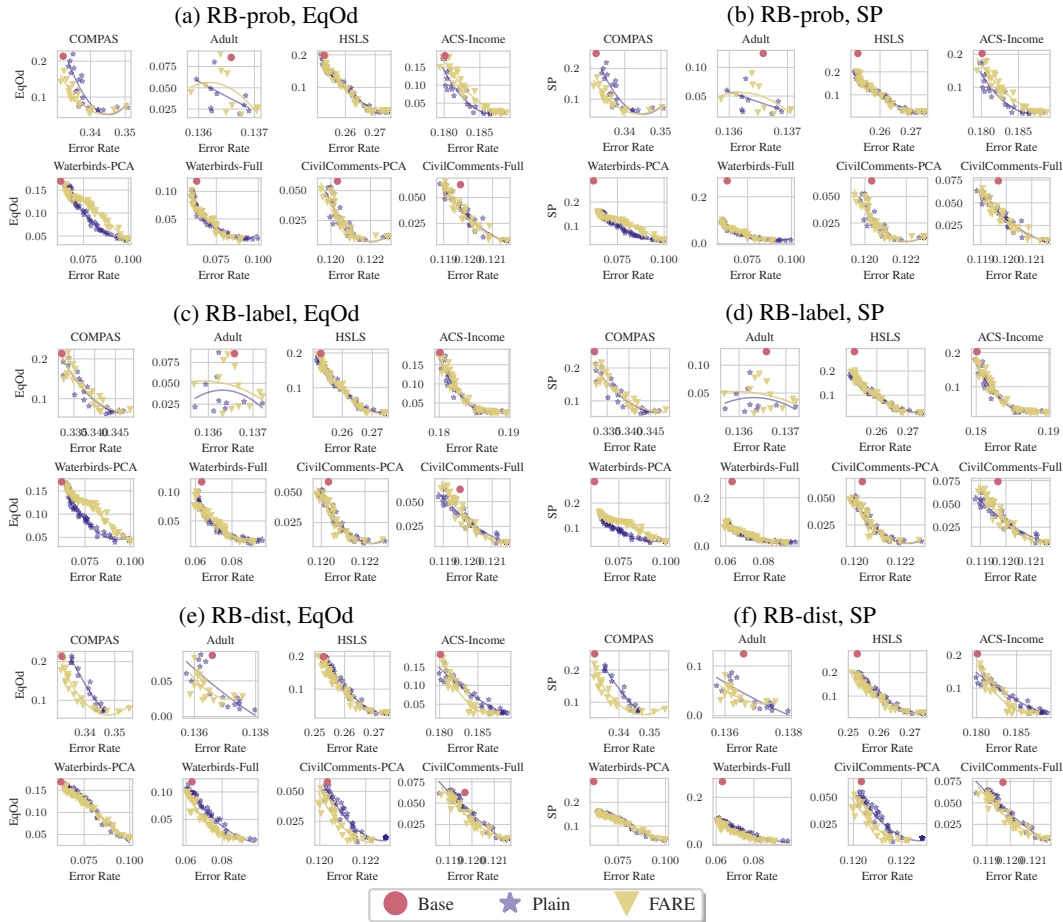


Figure 15: The Pareto fronts for using a fair representation when computing the KNN for RB-dist dominate the Pareto fronts for KNN computed on untransformed features. The blue stars represent the KNN without transforming the data, and the yellow triangles represent the KNN when the data is transformed using FARE (Jovanović et al., 2023). The lines are fitted by a polynomial of degree 2 to guide the eye.